A mesoscopic model for thermal–solutal problems of power-law fluids through porous media

Cite as: Phys. Fluids **33**, 033114 (2021); https://doi.org/10.1063/5.0042526
Submitted: 31 December 2020 . Accepted: 02 March 2021 . Published Online: 29 March 2021

Gholamreza Kefayati, Ali Tolooiyan, Andrew P. Bassom, and Kambiz Vafai

Physics of Fluids ARTICLE scitation.org/journal/phf

A mesoscopic model for thermal–solutal problems of power-law fluids through porous media

Cite as: Phys. Fluids **33**, 033114 (2021); doi: 10.1063/5.0042526
Submitted: 31 December 2020 · Accepted: 2 March 2021 ·
Published Online: 29 March 2021

View Online Export Citation CrossMark

Gholamreza Kefayati,[1,a)] Ali Tolooiyan,[1] Andrew P. Bassom,[2] and Kambiz Vafai[3]

AFFILIATIONS

[1]School of Engineering, University of Tasmania, Hobart 7001, Tasmania, Australia
[2]School of Natural Sciences, University of Tasmania, Hobart 7001, Tasmania, Australia
[3]Mechanical Engineering Department, University of California, Riverside, California 92521, USA

Note: This paper is part of the Special Issue on the Lattice Boltzmann Method.
[a)]**Author to whom correspondence should be addressed:** gholamreza.kefayati@utas.edu.au

ABSTRACT

A mesoscopic method based on the lattice Boltzmann method for thermal–solutal incompressible non-Newtonian power-law fluids through porous media is introduced. The macroscopic equations of different representative element volume (REV) models of porous media are presented, and the equations of power-law fluids through porous media for various REV models reported. The general mesoscopic model for two- and three-dimensional cases are presented, and their derivations shown. To demonstrate the ability of the proposed method, natural convection and double-diffusive natural convection of Newtonian and power-law fluids in porous cavities are studied, and the results are validated against previous findings. Finally, double-diffusive natural convection in a porous cubic cavity filled with a non-Newtonian power-law fluid is simulated by the proposed method.

I. INTRODUCTION

The study of fluid flow, heat, and mass transfer through porous media has been important for centuries, and significant efforts have been devoted for modeling and simulation of the material continuously.[1–4] Some of the engineering applications at which the heat and mass transfer through porous media plays a key role are geophysics, die filling, metal processing, agricultural and industrial water distribution, oil recovery techniques, injection molding, and hyperthermia on cancer cells. To study fluid flow, heat, and mass transfer in the porous medium, two general methods of the pore-scale approach and the representative element volume (REV) scale approach are generally considered. The pore-scale method is complicated to apply and demands significant computer resources. In contrast, the REV approach is more computationally efficient due to the application of the average transport properties and more straightforward to implement. The background and the development process of REV models for Newtonian fluids are presented and discussed in Appendix A.[1–25] However, most fluids and the interaction of some fluids with porous structures in natural and industrial applications, e.g., biofluidics,[26] geophysics,[27] biomechanical studies,[28,29] hydraulic fracturing,[30] and enhanced oil recovery[31] show non-Newtonian behavior.[32] So, the Newtonian models can lead to incorrect predictions of flow, heat, and mass transfer for these kinds of complex porous medium systems. Studying non-Newtonian fluid flow through porous media has been received significant attention and investigated by researchers from different disciplines of science and engineering for a long time. Some of the earlier review articles and developments can be found in the studies by Bird *et al.*,[33] Christopher and Middleman,[34] Savins,[35] Kemblowski and Michniewicz,[36] Pascal,[37] Dharmadhikari and Kale[38] where they applied non-Newtonian power-law model in the Darcy model. In the power-law model, the shear rate dependent viscosity is given by $\eta(\dot{\gamma}) = \mu^* \dot{\gamma}^{(n-1)}$ where μ^* and n are the consistency and power law indices and $\dot{\gamma}$ is the shear rate defined by $\dot{\gamma} = \frac{1}{\sqrt{2}} \sqrt{\mathbf{A_1} : \mathbf{A_1}}$. The power-law model is considered as a subclass of generalized Newtonian fluids and the constitutive equation for this kind of fluid is $\boldsymbol{\tau} = \eta(\dot{\gamma})\mathbf{A_1}$ where $\boldsymbol{\tau}$ is the extra stress tensor. A power-law index of $0 < n < 1$ represents a shear-thinning fluid, while $n > 1$ exhibits that the fluid is shear-thickening and $n = 1$ results in the Newtonian fluid. The modified Darcy's law in the presence of gravity force effect can be written as

$$\nabla p = \rho \mathbf{g} - \left[\frac{\mu^* |\mathbf{u}|^{(n-1)}}{K^*}\right] \mathbf{u}, \tag{1}$$

where K^* is the modified permeability and defined by a relation based on porosity, power-law index, and constant parameters as

$$K^* = \frac{1}{2C_t}\left(\frac{n\epsilon}{3n+1}\right)^n \left(\frac{50K}{3\epsilon}\right)^{(n+1)/2}, \tag{2}$$

C_t which is the tortuosity factor found differently by various authors. Christopher and Middleman[34] proposed $C_t = \frac{25}{12}$, Kemblowski and Michniewicz[36] suggested $C_t = 2.5^n\, 2^{(1-n)/2}$, Pascal[37] showed $C_t = \left(\frac{25}{12}\right)^{(n+1)/2}$, and Dharmadhikari and Kale[38] expressed it as

$$C_t = \frac{2}{3}\left(\frac{8n}{9n+3}\right)^n \left(\frac{10n-3}{6n+1}\right)\left(\frac{75}{16}\right)^{\frac{3(10n-3)}{(10n+11)}}. \tag{3}$$

Based on their empirical results, Dharmadhikari and Kale[38] introduced a new power-law index in Eq. (3) by $n' = n + 0.3(1-n)$. They indicated the main reason for the updated power-law index is the different behavior of power-law fluid flows through porous media where they incline to have a shorter path because of the stretching and contracting deformation which causes the tortuosity factor to lower values in shear-thinning fluids compared to Newtonian fluids.

The extended Darcy model for power-law fluids was studied by several researchers in various problems.[39–47] In some previous studies, the Forchheimer term also considered for analyzing the porous media. Shenoy[48] derived the governing equation for Darcy–Forchheimer flow of non-Newtonian power-law fluids through porous media, using the approximate integral method. They used the obtained equations for studying the forced and mixed convection heat transfer in non-Newtonian power-law fluid-saturated porous media as follows:

$$\nabla p = \rho \mathbf{g} - \left(\frac{\mu^* |\mathbf{u}|^{(n-1)}}{K^*} + \frac{E\,\rho\,|\mathbf{u}|}{\sqrt{K}}\right)\mathbf{u}. \tag{4}$$

Shenoy[49] considered the effect of Brinkman part and extended the Brinkman–Darcy equation for power-law fluids. It was indicated that the Brinkman term is valid in high porosities so it is safe and reasonable to assume the dynamic viscosity shows the non-Newtonian power-law behavior as

$$\nabla p = \rho \mathbf{g} + \frac{\mu^*}{\epsilon^n}\nabla \cdot \left[\dot{\gamma}^{(n-1)}\,\mathbf{A_1}\right] - \left(\frac{\mu^* |\mathbf{u}|^{(n-1)}}{\bar{K}^*}\right)\mathbf{u}. \tag{5}$$

Shenoy[49] showed the complete form of the equation of general non-Darcy flow of power-law fluids including the inertia and Brinkman terms as

$$\frac{\rho}{\epsilon^2}(\mathbf{u}\cdot\nabla\mathbf{u}) = \rho\mathbf{g} - \nabla p + \frac{\mu^*}{\epsilon^n}\nabla\cdot\left[\dot{\gamma}^{(n-1)}\,\mathbf{A_1}\right] - \left(\frac{\mu^*|\mathbf{u}|^{(n-1)}}{K^*} + \frac{E\,\rho\,|\mathbf{u}|}{\sqrt{K}}\right)\mathbf{u}. \tag{6}$$

Although Eq. (6) is restricted to high porosity regions, the models of Darcy, Darcy–Forchheimer, and Brinkman–Darcy can be obtained from the equation with ignoring the applied terms.

The main aim of this study is to introduce an lattice Boltzmann method (LBM) for thermal–solutal problems of non-Newtonian fluids through porous media which can recover the continuum, momentum, energy and concentration equations for the generalized porous model and non-Newtonian subclass of power-law model. In addition, the model has the ability to remove present limitations in simulating non-Newtonian fluids in conventional LBM. Following the development of the method, in Sec. II, two- and three-dimensional models of the approach in various REV porous models for the non-Newtonian power-law fluids are derived in thermal–solutal problems. In Sec. III, the proposed approach is evaluated with previous studies and applied for two- and three-dimensional thermal and thermal–solutal problems.

II. THE NUMERICAL METHOD

The lattice Boltzmann method (LBM) has been recognized as a powerful mesoscopic numerical method and alternative technique to macroscopic numerical approaches for simulation of different complex fluid flow, heat, and transfer problems.[50–58] The main benefits of LBM are the nature of the parallel algorithm, the simple and straightforward programming and implementation, and strong ability for complex geometries. In contrast to the common macroscopic numerical methods (e.g., the finite element method) which discretizes continuum equations, LBM utilizes mesoscopic kinetic equations which satisfy the macroscopic averaged properties. LBM is based on the movement of particles that are defined in specific directions in a selected lattice. So, it causes the computation process to drop significantly compared to microscopic methods. The basic information about conventional LBM and its previous models for studying non-Newtonian fluids and porous media is provided and discussed in Appendix B (Refs. 59–79), which clarifies the present gaps clearly.

The basic and fundamental concepts of the applied mesoscopic method in this study were initially introduced by Fu *et al.*[80,81] They presented a two-dimensional LBM which was combined with finite difference method and proposed a different equilibrium particle distribution function compared to conventional LBM based on a quadratic in the particle velocity. They also used a splitting technique to solve lattice Boltzmann equation (LBE) and set the non-dimensional relaxation time equal to one and extract the extra stress independent from the relaxation time. So, it makes this method appropriate for various non-Newtonian fluids. Fu *et al.*[80] validated the method with some basic benchmarks and was implemented for simulation of microchannel and microtube flows. The method was extended for thermal problems and presence of body forces in the study of Fu *et al.*[82] where they validated the proposed method with the case of two and three dimensional of natural convection in cavities which were filled with Newtonian fluid (air). However, in the studies of Fu *et al.*,[80–82] the derivation of all parameters in continuum momentum and energy equations were not shown properly and some elements in the equations, e.g., viscous dissipation, heat sources, or radiation were missed. Huilgol and Kefayati[83] removed the mentioned drawbacks and noted the equilibrium particle distribution function in the forms of vectors and matrices for two- and three-dimensional cases. They also developed the method for compressible flows. Then, Huilgol and Kefayati[84] developed the method for cylindrical and spherical coordinates. They validated the method with the lid-driven cavity and natural convection of Bingham fluid in a two-dimensional enclosure. In the next step, they used cylindrical coordinates for simulation of Bingham fluid and the Herschel–Bulkley fluid in a pipe of circular cross section and compared the obtained results with the numerical solutions of previous studies based on the discussed Lagrangian method. Kefayati *et al.*[85] developed thermal incompressible non-Newtonian fluids through porous media for two-dimensional cases. They assessed the accuracy of the method with studying natural convection in a porous cavity and

compared against previous papers. To show the ability of the proposed model, natural convection of power-law and Bingham fluids in a porous cavity were simulated.

In Eq. (6), which shows the generalized steady porous equation for power-law fluids, the term of Brinkman that represents the viscous shear stress can be presented with an extra stress tensor $\boldsymbol{\tau}$. So, the unsteady generalized equation can be written as

$$\frac{\rho}{\epsilon}\left[\frac{\partial \mathbf{u}}{\partial t}+(\mathbf{u}\cdot\nabla)\frac{\mathbf{u}}{\epsilon}\right]=\rho\mathbf{g}-\nabla p+\frac{1}{\epsilon^{n}}\nabla.\boldsymbol{\tau}-\left(\frac{\mu^{*}|\mathbf{u}|^{(n-1)}}{K^{*}}+\frac{E\rho|\mathbf{u}|}{\sqrt{K}}\right)\mathbf{u}. \tag{7}$$

In the presence of an external force $\mathbf{F}'$, e.g., gravity force ($\rho\mathbf{g}$) and multiplying two sides of Eq. (7) by porosity ϵ, we have

$$\rho\left[\frac{\partial \mathbf{u}}{\partial t}+(\mathbf{u}\cdot\nabla)\frac{\mathbf{u}}{\epsilon}\right]=-\nabla(\epsilon p)+\frac{1}{\epsilon^{(n-1)}}\nabla.\boldsymbol{\tau}+\mathbf{F}, \tag{8}$$

$$\mathbf{F}=-\frac{\epsilon\mu^{*}|\mathbf{u}|^{(n-1)}}{K^{*}}\mathbf{u}-\frac{\rho E\epsilon}{\sqrt{K}}|\mathbf{u}|\mathbf{u}+\epsilon\mathbf{F}'. \tag{9}$$

In this approach, the applied normalized Boltzmann equation in the presence of the external forces is similar to the LBE with the Bhatnagar–Gross–Krook (BGK) approximation which is presented in Eq. (B14). In contrast to the shown equilibrium distribution function in Eq. (B16), the $f_i^{eq}(\mathbf{x},t)$ is found as

$$f_i^{eq}(\mathbf{x},t)=K_i+\mathbf{e_i}\cdot\mathbf{L}_i+(\mathbf{e_i}\otimes\mathbf{e_i}):\mathbf{M}_i. \tag{10}$$

To satisfy the generalized equation of incompressible porous media or Darcy–Forchheimer–Brinkman equation for a two-dimensional case with the lattice of D2Q9, the scalar parameter K_i, the vector $\mathbf{L_i}$, and the symmetric matrix $\mathbf{M_i}$ are calculated by (see Appendix C)

$$K_0=\rho-\frac{2p\epsilon}{c^2}-\frac{\rho|\mathbf{u}|^2}{c^2}+\frac{\tau_{xx}+\tau_{yy}}{\epsilon^{(n-1)}c^2}, \tag{11a}$$

$$K_i=0,\quad i=1,2,\ldots,8, \tag{11b}$$

$$\mathbf{L}_1=\frac{\rho\mathbf{u}}{2c^2}=\mathbf{L}_i,\quad i=1,3,5,7 \tag{11c}$$

$$\mathbf{L}_i=\mathbf{0},\quad i=0,2,4,6,8 \tag{11d}$$

$$\mathbf{M}_1=\begin{bmatrix}M_{11}&0\\0&M_{22}\end{bmatrix}, \tag{11e}$$

$$M_{11}=\frac{1}{2c^4}\left[\epsilon p+\rho\left(\frac{u^2}{\epsilon}\right)-\frac{1}{\epsilon^{(n-1)}}\tau_{xx}\right], \tag{11f}$$

$$M_{22}=\frac{1}{2c^4}\left[\epsilon p+\rho\left(\frac{v^2}{\epsilon}\right)-\frac{1}{\epsilon^{(n-1)}}\tau_{yy}\right], \tag{11g}$$

$$\mathbf{M}_2=\begin{bmatrix}0&M_{12}\\M_{21}&0\end{bmatrix}, \tag{11h}$$

$$M_{12}=M_{21}=\frac{1}{8c^4}\left[\rho\left(\frac{uv}{\epsilon}\right)-\frac{1}{\epsilon^{(n-1)}}\tau_{xy}\right]. \tag{11i}$$

It should be noted that the matrices $\mathbf{M}_i$ are such that $\mathbf{M}_0=0$; $\mathbf{M}_1=\mathbf{M}_i$, $i=1,3,5,7$; $\mathbf{M}_2=\mathbf{M}_i$, $i=2,4,6,8$. The force term (F_i) in Eq. (B14) can be calculated by

$$F_i=\frac{1}{2c^2}\mathbf{F}\cdot\mathbf{e}_i,\quad i=1,3,5,7 \tag{12a}$$

$$F_i=0,\quad i=0,2,4,6,8. \tag{12b}$$

In this method, a splitting method[86] is used to solve the equation of lattice Boltzmann–BGK (LBGK) (B14). It is possible to separate the equation into two parts of streaming and collision as

$$\frac{\partial f_i}{\partial t}+\mathbf{e_i}\cdot\nabla_{\mathbf{x}}f_i-F_i=0\quad\text{streaming}, \tag{13}$$

$$\frac{\partial f_i}{\partial t}=\frac{-1}{\varpi_f}\left(f_i-f_i^{eq}\right)\quad\text{collision}. \tag{14}$$

The streaming part in Eq. (13) can be simplified in a discretization scheme as

$$f_i(\mathbf{x}+\mathbf{e_i}\Delta x,t+\Delta t)-f_i(\mathbf{x},t)-F_i(\mathbf{x},t)\,\Delta t=0 \tag{15}$$

and the collision part in Eq. (14) using the Euler method can be written in a discretized form as

$$f_i(\mathbf{x},t+\Delta t)=f_i^{eq}(\mathbf{x},t). \tag{16}$$

In contrast to the conventional LBM, boundary conditions are imposed directly with macroscopic values, which makes it one of the main advantage of this LBM. So, the boundary conditions are used as initial values (e.g., $\mathbf{u}$, p) in the parameters of the equilibrium distribution function (f_i^{eq}) in Eqs. (11a)–(11h). Then, the obtained f_i^{eq} are used to calculate the distribution function f_i in the collision part by applying Eq. (16). Next, in the streaming procedure which is considered in Eq. (15), f_i in the nearest particles in the lattice are found. Finally, the macroscopic values are updated with the obtained f_i in the previous step as

$$\mathbf{u}\equiv\frac{1}{\rho}\sum_{i=0}^{8}f_i\mathbf{e}_i, \tag{17}$$

$$p\equiv\sum_{i=0}^{8}f_i|\mathbf{e}_i|^2-\frac{1}{2\epsilon}\rho|\mathbf{u}|^2+\frac{\tau_{xx}+\tau_{yy}}{2\epsilon^{n}}, \tag{18}$$

and the algorithm repeats again from the cited initial step with the new f_i^{eq} as a result of the updated macroscopic values.

In order to satisfy the presented energy equation (A7) for thermal–solutal problems, the following equation based on energy distribution function is applied (see Appendix D).

$$\frac{\partial g_i}{\partial t}+\mathbf{e_i}\cdot\nabla_{\mathbf{x}}g_i-G_i=\frac{-1}{\varpi_g}\left(g_i-g_i^{eq}\right), \tag{19}$$

where the energy equilibrium distribution function $g_i^{eq}(\mathbf{x},t)$ has a linear relationship with the particle velocity as

$$g_i^{eq}(\mathbf{x},t)=A_i+\mathbf{e_i}\cdot\mathbf{B}_i, \tag{20}$$

the parameter A_i for various particles in D2Q9 lattice is calculated by $A_0=(\rho c_p)_m\,T$, $A_i=0; i=1,2,\ldots,8$. The vector $\mathbf{B}_i$ is defined as

$$\mathbf{B}_i=\frac{1}{2c^2}\left[(\rho c_p)_f\,\mathbf{u}\,T+\mathbf{q}+\mathbf{q}'-\boldsymbol{\tau}\cdot\mathbf{u}\right],\quad i=1,3,5,7 \tag{21}$$

where the heat flux ($\mathbf{q}$) follows the Fourier's law of heat conduction with effective thermal conductivity by $\mathbf{q}=-k_e\frac{\partial T}{\partial \mathbf{x}}$ and $\mathbf{q}'$ refers to the Dufour effect and is a heat flux due to a concentration gradient and is calculated by $\mathbf{q}'=-\frac{\rho D k_T}{c_s}\frac{\partial C}{\partial \mathbf{x}}$. For $i=0,2,4,6,8$, we have $\mathbf{B}_i=0$. The source term of G_i which is a scalar value is determined by

$$G_i = \left[\frac{\mu}{K}\,\mathbf{u} + \frac{\rho\, E}{\sqrt{K}}\,\mathbf{u}|\mathbf{u}|\right]\cdot\mathbf{u} + (\nabla\cdot\boldsymbol{\tau})\cdot\mathbf{u}\,, \quad i = 1,3,5,7 \tag{22}$$

and for $i = 0, 2, 4, 6, 8$, $G_i = 0$. The same splitting approach of f_i is applied for solving the equation of energy distribution function where the streaming and collision parts are found by $\frac{\partial g_i}{\partial t} + \mathbf{e_i}\cdot\nabla_{\mathbf{x}} g_i - G_i = 0$ and $\frac{\partial g_i}{\partial t} = \frac{-1}{\varpi_g}(g_i - g_i^{eq})$; respectively. The discretized form of the two parts after evaluation are obtained by $g_i(\mathbf{x} + \mathbf{e_i}\Delta x, t + \Delta t) - g_i(\mathbf{x}, t) - G_i(\mathbf{x}, t)\,\Delta t = 0$ and $g_i(\mathbf{x}, t + \Delta t) = g_i^{eq}(\mathbf{x}, t)$. The boundary conditions $(\mathbf{u_0}, p_0, T_0, C_0)$ provide the initial values for g_i^{eq}, so the values give the initial number of the equilibrium energy distribution function $(g_i^{0,eq})$ and updates the g_i in the collision part. In the streaming step, the g_i in the neighbor particles with the lattice space of Δx is obtained. Finally, the new value of temperature is calculated by

$$T \equiv \sum_{i=0}^{8} g_i(\mathbf{x}, t). \tag{23}$$

The found temperature from Eq. (23) can be implemented in the energy equilibrium distribution function for the next iteration $(g_i^{1,eq})$ and the process continues again from the collision part.

The macroscopic concentration equation is derived from a concentration distribution function as follows (see Appendix E):

$$\frac{\partial h_i}{\partial t} + \mathbf{e_i}\cdot\nabla_{\mathbf{x}} h_i = \frac{-1}{\varpi_h}\left(h_i - h_i^{eq}\right). \tag{24}$$

The concentration equilibrium distribution function $h_i^{eq}(\mathbf{x}, t)$ has a similar relationship to the energy one as

$$h_i^{eq}(\mathbf{x}, t) = Z_i + \mathbf{e_i}\cdot\mathbf{U}_i. \tag{25}$$

The scalar value of Z_i is found in various particles of the lattice by $Z_0 = \epsilon\, C$, $Z_i = 0; i = 1, 2, \ldots, 8$. The vector $\mathbf{U}_i$ is calculated as

$$\mathbf{U}_i = \frac{1}{2c^2}\left(\mathbf{J} + \mathbf{J}'\right), \quad i = 1,3,5,7 \tag{26}$$

where $(\mathbf{J})$ is the total mass flux, which is the combination of the advective $(\mathbf{J_a})$ and the diffusive or dispersive $(\mathbf{J_d})$ mass fluxes. $\mathbf{J_d}$ is defined by Fick's law as $\mathbf{J_d} = -D_e\nabla C$. The advective mass transfer is obtained by $\mathbf{J_a} = \mathbf{u}\,C$. $\mathbf{J}'$ is the thermo-diffusive mass fluxes and refers to the Soret parameter and is calculated by $\mathbf{J}' = -D_{CT}\nabla T$. For $i = 0, 2, 4, 6, 8$, we have $\mathbf{U}_i = 0$. The splitting method generates the streaming and collision sections in the forms of $\frac{\partial h_i}{\partial t} + \mathbf{e_i}\cdot\nabla_{\mathbf{x}} h_i = 0$ and $\frac{\partial h_i}{\partial t} = \frac{-1}{\varpi_h}(h_i - h_i^{eq})$; respectively. The discretized forms of the two parts after evaluation are obtained by $h_i(\mathbf{x} + \mathbf{e_i}\Delta x, t + \Delta t) - h_i(\mathbf{x}, t) = 0$ and $h_i(\mathbf{x}, t + \Delta t) = h_i^{eq}(\mathbf{x}, t)$. The boundary conditions give the initial values of h_i^{eq} and then updates the h_i in the collision part. In the streaming step, the h_i in the neighbor particles with the lattice space of Δx is found. Consequently, the new value of concentration is calculated by

$$C \equiv \sum_{i=0}^{8} h_i(\mathbf{x}, t). \tag{27}$$

The value of concentration from Eq. (27) is implemented in the concentration equilibrium distribution function in the next iteration $(h_i^{1,eq})$.

A. Three-dimensional models

Different space-filling, symmetric lattices can be used for three-dimensional cases in this method. Here, the D3Q15 lattice is implemented. The applied LBE and the equilibrium distribution function are similar to Eqs. (B14) and (10), respectively. The parameters in Eq. (10) can be calculated as

$$K_0 = \rho - \frac{3p\epsilon}{c^2} - \frac{\rho|\mathbf{u}|^2}{c^2} + \frac{\tau_{xx} + \tau_{yy} + \tau_{zz}}{\epsilon^{(n-1)}c^2}, \tag{28a}$$

$$K_i = 0, \quad i = 1, 2, \ldots, 14 \tag{28b}$$

$$\mathbf{L}_1 = \frac{\rho\mathbf{u}}{2c^2} = \mathbf{L}_i, \quad i = 1, \ldots, 6 \tag{28c}$$

$$\mathbf{L}_i = \mathbf{0}, \quad i = 0, 7, 8, \ldots, 14 \tag{28d}$$

$$\mathbf{M}_1 = \begin{bmatrix} M_{xx} & 0 & 0 \\ 0 & M_{yy} & 0 \\ 0 & 0 & M_{zz} \end{bmatrix}, \tag{28e}$$

$$M_{xx} = \frac{1}{2c^4}\left[\epsilon p + \rho\left(\frac{u^2}{\epsilon}\right) - \frac{1}{\epsilon^{(n-1)}}\tau_{xx}\right], \tag{28f}$$

$$M_{yy} = \frac{1}{2c^4}\left[\epsilon p + \rho\left(\frac{v^2}{\epsilon}\right) - \frac{1}{\epsilon^{(n-1)}}\tau_{yy}\right], \tag{28g}$$

$$M_{zz} = \frac{1}{2c^4}\left[\epsilon p + \rho\left(\frac{w^2}{\epsilon}\right) - \frac{1}{\epsilon^{(n-1)}}\tau_{zz}\right], \tag{28h}$$

$$\mathbf{M}_2 = \begin{bmatrix} 0 & M_{xy} & M_{xz} \\ M_{yx} & 0 & M_{yz} \\ M_{zx} & M_{zy} & 0 \end{bmatrix}, \tag{28i}$$

$$M_{xy} = M_{yx} = \frac{1}{8c^4}\left[\rho\left(\frac{uv}{\epsilon}\right) - \frac{1}{\epsilon^{(n-1)}}\tau_{xy}\right], \tag{28j}$$

$$M_{yz} = M_{zy} = \frac{1}{8c^4}\left[\rho\left(\frac{vw}{\epsilon}\right) - \frac{1}{\epsilon^{(n-1)}}\tau_{yz}\right], \tag{28k}$$

$$M_{xz} = M_{zx} = \frac{1}{8c^4}\left[\rho\left(\frac{uw}{\epsilon}\right) - \frac{1}{\epsilon^{(n-1)}}\tau_{xz}\right]. \tag{28l}$$

It should be noted that the matrices $\mathbf{M}_i$ are such that $\mathbf{M}_0 = 0$; $\mathbf{M}_1 = \mathbf{M}_i$, $i = 1, \ldots, 6$; $\mathbf{M}_2 = \mathbf{M}_i$, $i = 0, 7, \ldots, 14$.

The equilibrium distribution function is modified as follows:

$$\sum_{\alpha=0}^{14} f_\alpha^{\mathrm{eq}} = \rho, \tag{29}$$

$$\sum_{\alpha=0}^{14} f_\alpha^{\mathrm{eq}}\boldsymbol{\xi}_\alpha = \rho\mathbf{u}, \quad \mathbf{u} = u\mathbf{i} + v\mathbf{j} + w\mathbf{k}, \tag{30}$$

$$\sum_{\alpha=0}^{14} f_\alpha^{\mathrm{eq}}\boldsymbol{\xi}_\alpha \otimes \boldsymbol{\xi}_\alpha = \mathbf{M}, \tag{31}$$

$$\sum_{\alpha=0}^{14} f_\alpha^{(n)} = 0, \quad n \geq 1, \tag{32}$$

$$\sum_{\alpha=0}^{14} f_\alpha^{(n)}\boldsymbol{\xi}_\alpha = 0, \quad n \geq 1, \tag{33}$$

where $\mathbf{M}$ has the matrix form as

$$\mathbf{M} = \begin{bmatrix} M_{xx} & M_{xy} & M_{xz} \\ M_{yx} & M_{yy} & M_{yz} \\ M_{zx} & M_{zy} & M_{zz} \end{bmatrix}. \tag{34}$$

The body force distribution functions now satisfy

$$\sum_{i=0}^{14} F_i = 0\,, \quad \sum_{i=0}^{14} F_i \mathbf{e}_i = \mathbf{F}. \tag{35}$$

The choice of F_i in different particles in the lattice is

$$F_0 = 0, \quad F_1 = \frac{1}{2c^2}\mathbf{F}\cdot\mathbf{e}_1 = -F_3, \tag{36}$$

$$F_2 = \frac{1}{2c^2}\mathbf{F}\cdot\mathbf{e}_2 = -F_4, \tag{37}$$

$$F_5 = \frac{1}{2c^2}\mathbf{F}\cdot\mathbf{e}_5 = -F_6, \tag{38}$$

$$F_i = 0, \quad i = 7, \ldots, 14. \tag{39}$$

The energy distribution function in Eq. (19) and the energy equilibrium distribution function in Eq. (20) are utilized in the three-dimensional model while the following conditions should be satisfied

$$\sum_{i=0}^{14} g_i^{(n)} = 0, \quad n \geq 1, \tag{40}$$

$$\sum_{i=0}^{14} g_i^{eq} = (\rho c_p)_m\, T, \tag{41}$$

$$\sum_{i=0}^{14} g_i^{eq}\mathbf{e}_i = (\rho c_p)_f T\,\mathbf{u} + \mathbf{q} + \mathbf{q}' - \boldsymbol{\tau}\cdot\mathbf{u}, \tag{42}$$

$$\sum_{i=0}^{14} G_i = \left[\frac{\mu}{K}\mathbf{u} + \frac{\rho E}{\sqrt{K}}\mathbf{u}|\mathbf{u}|\right]\cdot\mathbf{u} + (\nabla\cdot\boldsymbol{\tau})\cdot\mathbf{u}, \tag{43}$$

where the parameters in Eq. (20) for g_i^{eq} are calculated as

$$A_0 = (\rho c_p)_m\, T\,; \quad A_i = 0\,; i = 1, 2, \ldots, 8. \tag{44}$$

The vector $\mathbf{B}_i$ is defined as

$$\begin{gathered} \mathbf{B}_i = \frac{1}{2c^2}\left[(\rho c_p)_f\,\mathbf{u}\,T + \mathbf{q} + \mathbf{q}' - \boldsymbol{\tau}\cdot\mathbf{u}\right], \quad i = 1, \ldots, 6 \\ \mathbf{B}_i = 0\,, \quad i = 0, 7, \ldots, 14. \end{gathered} \tag{45}$$

The source term of G_i in the three dimensional model is obtained as

$$\begin{gathered} G_i = \left[\frac{\mu}{K}\,\mathbf{u} + \frac{\rho\, E}{\sqrt{K}}\,\mathbf{u}|\mathbf{u}|\right]\cdot\mathbf{u} + (\nabla\cdot\boldsymbol{\tau})\cdot\mathbf{u}\,, \quad i = 1, \ldots, 6 \\ G_i = 0\,, \quad i = 0, 7, \ldots, 14. \end{gathered} \tag{46}$$

To find the concentration distribution function (h_i), Eq. (24) similar to the two-dimensional case is applied and also the equilibrium concentration distribution function (h_i^{eq}) follows Eq. (25) and need to satisfy the following conditions:

$$\sum_{i=0}^{14} h_i^{eq} = \epsilon C, \tag{47}$$

$$\sum_{i=0}^{14} h_i^{eq}\mathbf{e}_i = \mathbf{J} + \mathbf{J}'. \tag{48}$$

The scalar value of Z_i and the vector $\mathbf{U}_i$ in the equation is found by

$$\begin{gathered} Z_0 = \epsilon\, C, \quad Z_i = 0; \quad i = 1, 2, \ldots, 14 \\ \mathbf{U}_i = \frac{1}{2c^2}(\mathbf{J} + \mathbf{J}'), \quad i = 1, \ldots, 6 \\ \mathbf{U}_i = 0\,, \quad i = 0, 7, \ldots, 14. \end{gathered} \tag{49}$$

III. VALIDATION AND NUMERICAL EXAMPLES

Double-diffusive natural convection in a two-dimensional porous cavity with the height of H and the length of L which is filled with a Newtonian fluid ($\boldsymbol{\tau} = \mu_e\,\mathbf{A_1}$) was studied by Goyeau *et al.*[87] The horizontal walls of the enclosure have zero mass and heat fluxes while all vertical and horizontal walls are impermeable. The temperatures of the hot left wall and the cold right wall of the cavity were fixed at T_H, and T_C. The concentrations of the hot left wall and the cold right wall of the cavity were fixed at C_H, and C_C. They applied the Darcy and the Darcy–Brinkman models for the porous media and solved the generalized equations in the absence of the Forchheimer inertia term in the momentum equation by finite difference method (FDM) since they considered the values which resulted in Reynolds number less than unity. In their work, they assumed the fluid flow is incompressible and the parameters of viscous dissipation, Soret, and Dufour were neglected. They also assumed the effective viscosity (μ_e) and the effective thermal conductivity (k_e) in the Brinkman term is equal to the fluid viscosity (μ) and thermal conductivity (k). It causes the effective thermal exclusivity to become equal to the fluid thermal diffusivity ($\alpha = \alpha_e$) while Boussinesq approximation was implemented for change of density. So, the studied macroscopic dimensional equations for the Darcy–Brinkman model were used as

$$\nabla\cdot\mathbf{u} = 0, \tag{50}$$

$$\begin{aligned} \frac{\rho}{\epsilon^2}(\mathbf{u}\cdot\nabla)\,\mathbf{u} = -\nabla p + \mu_e\nabla^2\mathbf{u} - \frac{\mu}{K}\,\mathbf{u} \\ + \rho g[\beta_T(T - T_C) + \beta_C(C - C_C)]\mathbf{e_y}, \end{aligned} \tag{51}$$

$$\mathbf{u}.\nabla T = \alpha_e\nabla^2 T, \tag{52}$$

$$\mathbf{u}.\nabla C = D_e\nabla^2 C, \tag{53}$$

where $\mathbf{e_y}$ is the unit vector in the y direction. β_T and β_C are the thermal expansion coefficient and the concentration expansion coefficient, which are defined as

$$\beta_T = -\frac{1}{\rho}\left[\frac{\partial\rho}{\partial T}\right]_C \quad \text{and} \quad \beta_C = -\frac{1}{\rho}\left[\frac{\partial\rho}{\partial C}\right]_T. \tag{54}$$

It is needed to find the non-dimensional equations to solve the problem. Several researchers have endeavored to introduce specific non-dimensional variables to decrease the number of the non-dimensional variables (e.g., see the proposed methods by Refs. 88–90) Here, the non-dimensional variables of $x^* = \frac{\mathbf{x}}{H}$, $\mathbf{u}^* = \frac{\mathbf{u}}{U}$, $p^* = \frac{p}{\rho U^2}$, $T^* = (T - T_C)/\Delta T$, $\Delta T = T_H - T_C$, $C^* = (C - C_C)/\Delta C$, $\Delta C = C_H - C_C$, $\alpha_m = \frac{k_e}{\epsilon\,\rho\,cp_f}$ are applied to obtain non-dimensional equations. The buoyancy velocity scale (U) is found by $U = \left(\frac{\alpha_m}{H}\right) Ra_m^{0.5}$ where Ra_m is the modified Rayleigh number and calculated by $Ra_m = \frac{\rho^2\beta_T g H^3 \Delta T\, Pr_m}{\mu_e^2}$. The modified Prandtl number (Pr_m), Darcy number (Da_m) and Lewis number (Le_m) are defined by

$$Pr_m = \frac{\mu_e}{\alpha_m \rho}, \quad Da_m = \frac{K}{\epsilon H^2}, \quad Le_m = \frac{\alpha_m}{D_e}. \tag{55}$$

As a result, the non-dimensional equations after dropping the asterisks can be written as

$$\nabla \cdot \mathbf{u} = 0, \tag{56}$$

$$(\mathbf{u}\cdot\nabla)\,\mathbf{u} = -\nabla p + \frac{Pr_m}{\sqrt{Ra_m}}\nabla^2\mathbf{u} - \frac{Pr_m}{Da_m\sqrt{Ra_m}}\mathbf{u} + Pr_m(T+NC)\mathbf{e_y}, \tag{57}$$

$$\mathbf{u}.\nabla T = \frac{1}{\sqrt{Ra_m}}\nabla^2 T, \tag{58}$$

$$\mathbf{u}.\nabla C = \frac{1}{Le_m\sqrt{Ra_m}}\nabla^2 C, \tag{59}$$

where N is the buoyancy ratio which is defined by $N = \frac{\beta_C \Delta C}{\beta_T \Delta T}$. Goyeau *et al.*[87] fixed the Prandtl number at $Pr = \frac{\mu}{\rho\,\alpha} = 10$ and $\sigma = 1$ (in other words, they kept the porosity equal to unity ($\epsilon = 1$) and therefore the modified non-dimensional parameters are equal to the non-dimensional parameters in the study; $Le_m = Le$, $Ra_m = Ra$, and $Da_m = Da$). The non-dimensional parameters of the mesoscopic method for solving the non-dimensional macroscopic equations for a Newtonian fluid ($n = 1$) are needed to be found. Equations (11a)–(11i) are used for recovering the non-dimensional continuity equations where the non-dimensional extra tensor is calculated by $\boldsymbol{\tau} = \frac{Pr_m}{\sqrt{Ra_m}}\mathbf{A_1}$. The force term in Eq. (12a) is obtained by $\mathbf{F} = -\frac{Pr_m}{Da_m\sqrt{Ra_m}} + Pr_m(T+NC)$. For recovering the non-dimensional energy equation, the parameters in Eq. (20) are defined by $A_0 = T$; $\mathbf{B_i} = \frac{1}{2c^2}[\mathbf{u}T + \mathbf{q}]$ as the non-dimensional heat flux is implemented by $\mathbf{q} = -\frac{1}{\sqrt{Ra_m}}\nabla T$. To find the variables in Eq. (25) for having the dimensionless concentration, they are determined by $Z_0 = C$; $\mathbf{U_i} = \frac{1}{2c^2}[\mathbf{u}C - \frac{1}{Le_m\sqrt{Ra_m}}\nabla C]$. In this study, the time step is fixed at $\Delta t = 0.0001$ and the applied mesh is $\Delta x = \Delta y = 150$. The stopping criterion for this applied approach is as

$$\left|\rho - \sum_{i=0}^{8} f_i(\mathbf{x},\mathbf{t})\right| < (\Delta t)^2. \tag{60}$$

In fact, the algorithm continues until the specified difference between the sum of the distribution functions and the density.

Figure 1 compares the results of the present method and the work of Goyeau *et al.*[87] for isotherms, streamlines, and isoconcentrations at $Le = 10$, $N = 10$, $Da = 10^{-3}$, $Pr = 10$ and $Ra = 10^5$ (it should be noted that Goyeau *et al.*[87] used the term of $Ra^* = 100$ which has the following relationship $Ra = Ra^*/Da = 10^5$). The thermal Rayleigh number (Ra) and Darcy number (Da) were defined by $Ra = \frac{\rho g \beta_T \Delta T H^3}{\mu\alpha}$ and $Da = \frac{K}{H^2}$; respectively. They evaluated heat and mass transfer by calculating the average Nusselt (Nu) and Sherwood (Sh) numbers at the left hot wall as follows:

$$Nu = \int_0^1 \left[\frac{\partial T}{\partial x}\right]_{x=0} dy, \quad Sh = \int_0^1 \left[\frac{\partial C}{\partial x}\right]_{x=0} dy. \tag{61}$$

Sezai and Mohamad[91] studied the three-dimensional case of the above problem with opposing and horizontal gradients of temperature and concentration. They validated their two (2D) and three dimensional (3D) results with the study of Goyeau *et al.*[87] using the average Nusselt and Sherwood numbers. The average Nusselt (Nu) and Sherwood numbers (Sh) at the left hot wall are calculated as

$$Nu = \int_0^1\int_0^1 \left[\frac{\partial T}{\partial x}\right]_{x=0} dy\,dz, \tag{62}$$

$$Sh = \int_0^1\int_0^1 \left[\frac{\partial C}{\partial x}\right]_{x=0} dy\,dz. \tag{63}$$

For this problem, the time step is chosen by $\Delta t = 10^{-4}$ and the applied mesh is $\Delta x = \Delta y = \Delta z = \frac{1}{50}$. Figures 2 and 3 illustrate the average Nusselt and Sherwood numbers for two- and three-dimensional cases in different buoyancy ratios. The figures compare the results of the present method with the work of Sezai and Mohamad.[91] The comparison demonstrates a good agreement between the present study and the study of Sezai and Mohamad.[91] To validate the mesoscopic method for a thermal non-Newtonian fluids through porous media, a two-dimensional shallow porous cavity with the height of H and the length of L which is filled with power-law fluid for laminar, incompressible, and steady flow has been investigated. The problem was studied analytically and numerically by Bian *et al.*[94] The constant hot and cold temperatures on the vertical sides were used while the horizontal sides were insulated. They applied the modified Darcy model for the momentum equation [which is shown in Eq. (1)] and the Boussinesq approximation was applied. In addition, it was assumed the viscous dissipation is negligible. So, the governing equations of the study can be presented as

$$\nabla \cdot \mathbf{u} = 0, \tag{64}$$

$$0 = -\nabla p - \left[\frac{\mu^*|\mathbf{u}|^{(n-1)}}{K^*}\right]\mathbf{u} + \rho g \beta_T (T - T_C)\mathbf{e_y}, \tag{65}$$

$$\mathbf{u}.\nabla T = \alpha_e \nabla^2 T. \tag{66}$$

The modified permeability K^* is calculated based on Eq. (2) where the proposed value of Pascal[37] for the tortuosity factor ($C_t = (\frac{25}{12})^{(n+1)/2}$) is implemented. The non-dimensional variables for this problem were introduced in[94–97] as $x^* = \frac{x}{L}$, $\mathbf{u}^* = \frac{\mathbf{u}L}{\alpha}$, $p^* = \frac{p\,K\,L^{(n-1)}}{\alpha^n\,\mu^*}$, and $T^* = (T - T_C)/\Delta T^*$, $\Delta T^* = T_H - T_C$. With dropping asterisks, the non-dimensional equations were presented in the cited studies[92–97] as

$$\nabla \cdot \mathbf{u} = 0, \tag{67}$$

$$0 = -\nabla p - \left(|\mathbf{u}|^{(n-1)}\mathbf{u}\right) + R^*\,(T\mathbf{e_y}), \tag{68}$$

$$\mathbf{u}.\nabla T = \nabla^2 T, \tag{69}$$

where R^* is the modified Darcy–Rayleigh number which is given by $R^* = \frac{\rho\,\beta_T\,g\,K\,L^n\,\Delta T}{\mu^*\,\alpha^n}$. By taking the curl of Eq. (68), the pressure can also be eliminated.[92–97] With consideration to the definition of the curl operator, Eq. (68) can be altered to the following equation:

$$\nabla \times \left(|\mathbf{u}|^{(n-1)}\mathbf{u}\right) = R^*\,\nabla \times (T\mathbf{e_y}). \tag{70}$$

So, in the previous studies they solve Eq. (70) for the momentum equation. To apply the mesoscopic method, Eqs. (67)–(69) are considered. To solve the problem with mesoscopic method, the extra tensor ($\boldsymbol{\tau} = 0$) and the second-order velocities ($u^2 = v^2 = uv = 0$) in Eq. (11) are equal to zero and the porosity is also fixed at $\epsilon = 1$. The force

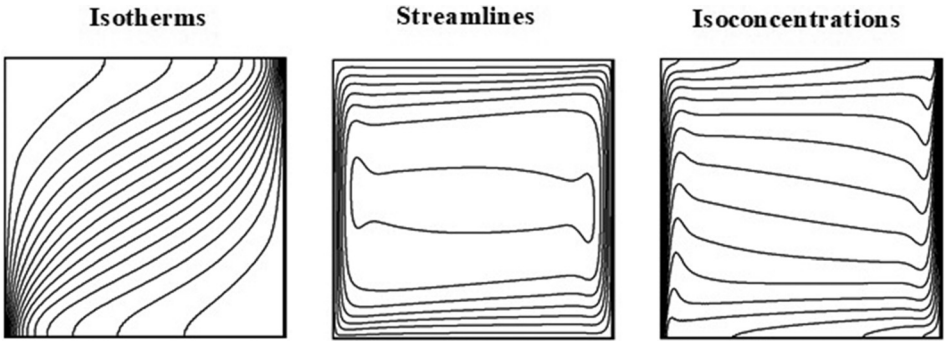

FIG. 1. Comparison between the present applied method and the result of Goyeau *et al.*[87] at $Le = 10$, $N = 10$, $Da = 10^{-3}$, $Pr = 10$, and $Ra = 10^5$.

term in Eq. (12a) is defined by $\mathbf{F} = -(|\mathbf{u}|^{(n-1)}\mathbf{u}) + R^*(T\mathbf{e_y})$. For recovering the energy equation, the parameters in Eq. (20) are implemented as $A_0 = T$; and $\mathbf{B_i} = \mathbf{u}T - \nabla T, \quad i = 1, 3, 5, 7$. To validate the results of the mesoscopic method with the presented analytical results of Bian *et al.*,[94] the average Nusselt number was compared for the aspect ratio of $A = H/L = 4$ in different modified Rayleigh–Darcy numbers and power-law indexes in Fig. 4. The shown lines in Fig. 4 are the obtained analytical results of Bian *et al.*[94] and the shown red symbols are the achieved values of the present mesoscopic method. The average Nusselt number was calculated as

$$Nu = \frac{1}{A}\int_0^A \left[\frac{\partial T}{\partial y}\right]_{y=0} dx. \tag{71}$$

Amari *et al.*[39] studied non-Newtonian power-law fluids through two-dimensional porous long shallow cavities while a constant heat flux (q') was applied on the bottom or side walls. The modified Darcy model was used for the momentum equation. The aspect ratio in the cavity was defined by $A' = L'/H'$ where L' and H' are the length and height of the cavity. The dimensional equation was similar to Eqs. (67)–(69). The non-dimensional variables were defined as $x^* = \frac{x}{H'}$, $\mathbf{u}^* = \frac{\mathbf{u}H'}{\alpha}$, $p^* = \frac{pKH'^{(n-1)}}{\alpha^n \mu^*}$, $T^* = (T - T_0)/\Delta T'$, and $\Delta T' = q'H'/k$. In this study, the average Nusselt number was computed by $Nu = \int_{-1/2}^{1/2} \left[\frac{1}{\Delta T}\right]_{x=0} dy$ where the ΔT is the dimensionless temperature difference. The applied mesoscopic method for this problem is the same as the previous problem and just the boundary conditions should be changed. The results are compared for the case of a bottom heated cavity for various power-law indexes and aspect ratios at $R^* = 100$ in Table I, which demonstrates a good agreement.

Khelifa[98] investigated double-diffusive natural convection in a vertical porous cavity filled with non-Newtonian power-law fluids numerically and analytically. The vertical walls of the cavity were subjected to constant fluxes of heat and solute and the two horizontal walls were impermeable and adiabatic. They also studied the effect of Soret parameter in the concentration equation and named this case Soret induced convection. They used the modified Darcy model of the momentum equation and applied the Boussinesq approximation for the density variation in temperature and concentration. Their non-dimensional governing equations can be written as[98,99]

$$\nabla \cdot \mathbf{u} = 0, \tag{72}$$

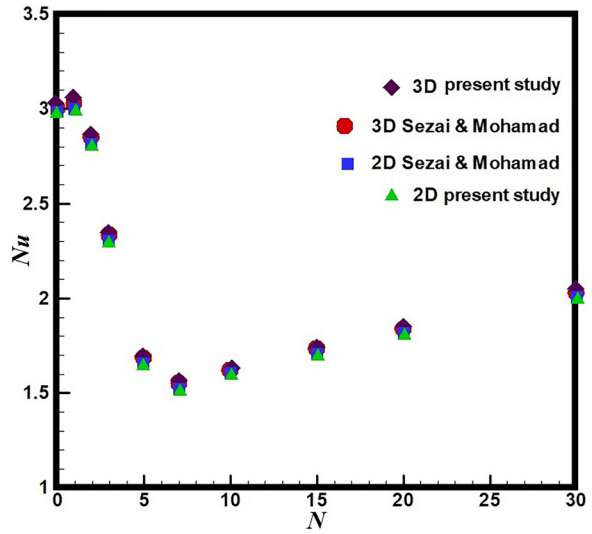

FIG. 2. Comparison of the average Nusselt number between the present applied method and the result of Sezai and Mohamad.[91]

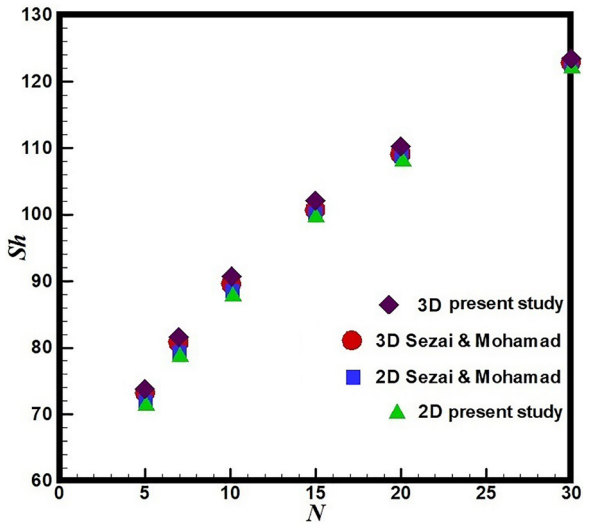

FIG. 3. Comparison of the average Sherwood number between the present applied method and the result of Sezai and Mohamad.[91]

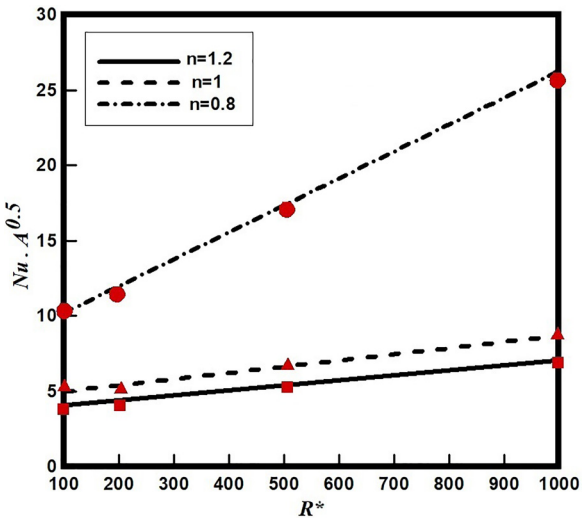

FIG. 4. Comparison of the average Nusselt number between the present applied method and the result of Bian *et al.*[94]

$$0 = -\nabla p - \left(|\mathbf{u}|^{(n-1)}\mathbf{u}\right) + R^*\,(T + NC)\,\mathbf{e_y}, \tag{73}$$

$$\frac{\partial T}{\partial t} + \mathbf{u}.\nabla T = \nabla^2 T, \tag{74}$$

$$\Lambda'\,\frac{\partial C}{\partial t} + \mathbf{u}.\nabla C = \frac{1}{Le}(\nabla^2 C - a\nabla^2 T). \tag{75}$$

They applied the same non-dimensional variables of the previous thermal example for the momentum and energy equation. The parameter Λ' was defined by $\Lambda' = \epsilon/\sigma$ and a was a constant number which played the role of the non-dimensional Soret parameter.

It should be noted that Khelifa[98] applied the Curl operation on the momentum to eliminate the pressure similar to the previous two examples. To apply the mesoscopic method for solving Eqs. (73)–(75), the approach is similar to the first example and the only difference is the force term which should be computed by $\mathbf{F} = -(|\mathbf{u}|^{(n-1)}\mathbf{u}) + R^*\,(T + NC)\mathbf{e_y}$. For recovering the concentration equation, the parameters in Eq. (25) are implemented as $Z_0 = \Lambda' C$; and $\mathbf{U_i} = \mathbf{u}C - \frac{1}{Le}(\nabla C - a\nabla T)\,, \quad i = 1, 3, 5, 7.$ The average Nusselt number and Sherwood number are compared with the study of Khelifa[98] in different buoyancy ratios and power-law indexes for $R^* = 100$, $Le = 10$, and $a = 0$ in Figs. 5 and 6.

In the next part, the three-dimensional power-law fluids in a porous cubic cavity have been studied by the method while the general equation of Brinkman–Forchheimer extended Darcy model has been applied. The dimensional equation with neglecting the viscous dissipation, Soret and Dufour parameters can be written as

$$\nabla \cdot \mathbf{u} = 0, \tag{76}$$

$$\frac{\rho}{\epsilon^2}\,(\mathbf{u}\cdot\nabla)\,\mathbf{u} = -\nabla p + \frac{1}{\epsilon^n}\,\nabla\cdot\boldsymbol{\tau} - \left(\frac{\mu^*|\mathbf{u}|^{(n-1)}}{K^*} + \frac{E\,\rho\,|\mathbf{u}|}{\sqrt{K}}\right)\mathbf{u} + \rho g[\beta_T(T - T_C) + \beta_C(C - C_C)]\mathbf{e_z}, \tag{77}$$

$$\mathbf{u}.\nabla T = \alpha_e \nabla^2 T, \tag{78}$$

$$\mathbf{u}.\nabla C = D_e \nabla^2 C, \tag{79}$$

where the extra tensor is $\boldsymbol{\tau} = \mu^*\dot{\gamma}^{(n-1)}\,\mathbf{A_1}$. Different velocity scales and non-dimensional methods have been applied for obtaining the non-dimensional equations of power-law fluids through natural convection process in enclosures[100–104] and porous cavities.[87–91,105] Here, the velocity scale is defined by $U = \sqrt{g\beta_T \Delta T L}$ where the parameter L is the length scale. With the cited scales, the non-dimensional parameters are calculated by $x^* = \frac{\mathbf{x}}{L}, \quad \mathbf{u}^* = \frac{\mathbf{u}}{U}, \quad p^* = \frac{p}{\rho U^2}\,, \boldsymbol{\tau}^* = \frac{\boldsymbol{\tau}}{\mu^*(\frac{U}{L})^n}\,, T^* = (T - T_C)/\Delta T, \quad \Delta T = T_H - T_C\,, C^* = (C - C_C)/\Delta C, \quad \Delta C = C_H - C_C$. So, the governing non-dimensional equations are presented as

$$\nabla \cdot \mathbf{u} = 0, \tag{80}$$

TABLE I. Comparison of the average Nusselt number between the present study and the results of Amari *et al.*[39] for a cavity heated from below in different power-law indexes and aspect ratios at $R^* = 100$.

	$n = 0.6$	$n = 1$	$n = 1.4$
$A' = 1$			
Present study	5.802	2.962	1.89
Amari *et al.*[39]	5.814	2.970	1.94
$A' = 2$			
Present study	5.66	3.59	2.48
Amari *et al.*[39]	5.75	3.63	2.51
$A' = 3$			
Present study	5.831	3.68	2.529
Amari *et al.*[39]	5.865	3.72	2.546
$A' = 4$			
Present study	5.981	3.699	2.51
Amari *et al.*[39]	5.997	3.708	2.55

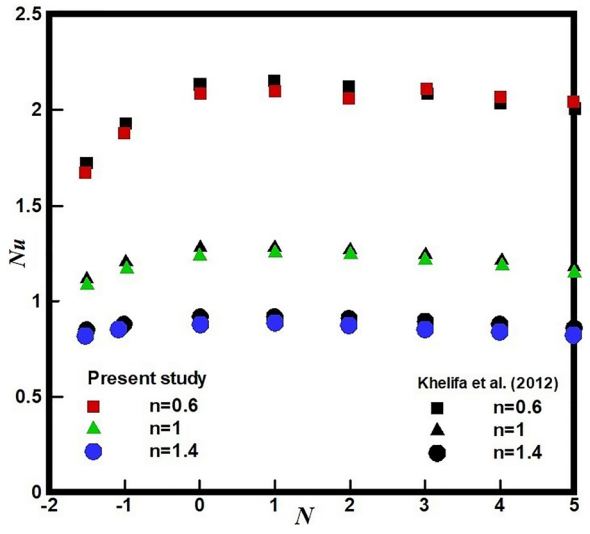

FIG. 5. Comparison of the average Nusselt number between the present applied method and the result of Khelifa *et al.*[98]

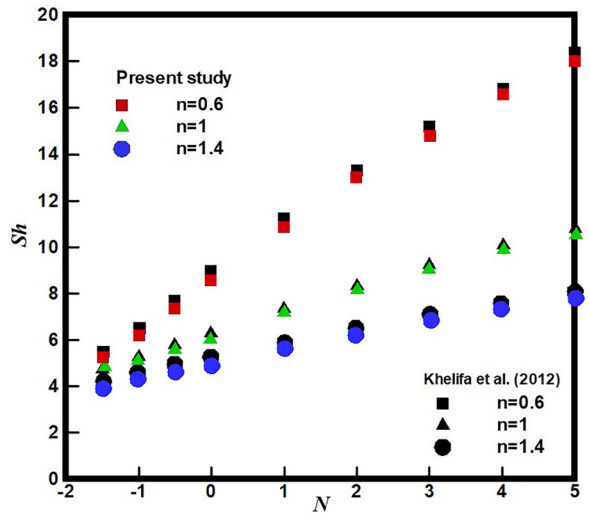

FIG. 6. Comparison of the average Sherwood number between the present applied method and the result of Khelifa *et al.*[98]

$$\frac{1}{\epsilon^2}(\mathbf{u}\cdot\nabla)\mathbf{u} = -\nabla p + \frac{1}{\epsilon^n\sqrt{Gr}}\nabla\cdot\boldsymbol{\tau} - \frac{E|\mathbf{u}|}{\sqrt{Da}}\mathbf{u} - \frac{|\mathbf{u}|^{(n-1)}}{K^{*\prime}Da\sqrt{Gr}}\mathbf{u} + (T+NC)\mathbf{e_z}, \tag{81}$$

$$\mathbf{u}.\nabla T = \frac{1}{Pr\,Gr^{\frac{1}{n+1}}}\nabla^2 T, \tag{82}$$

$$\mathbf{u}.\nabla C = \frac{1}{Le\,Pr\,Gr^{\frac{1}{n+1}}}\nabla^2 C, \tag{83}$$

where $K^{*\prime}$ is found by $K^{*\prime} = K^*/K$ and the dimensionless Grashof, Darcy, and Prandtl numbers are defined as

$$Gr = \frac{\rho^2 L^{n+2} g\,\beta_T\,\Delta T^{2-n}}{\mu^{*2}}, \quad Da = \frac{K}{L^2}, \tag{84}$$

$$Pr = \frac{1}{\alpha_e}\left(\frac{\mu^*}{\rho}\right)^{\left(\frac{2}{1+n}\right)} L^{\left(\frac{1-n}{1+n}\right)}(Lg\,\beta_T\,\Delta T)^{\frac{3(n-1)}{2(n+1)}}. \tag{85}$$

The non-dimensional extra tensor in the mesoscopic method in Eq. (28) is defined by $\boldsymbol{\tau} = \frac{1}{\epsilon\sqrt{Gr}}\mathbf{A_1}$. The force term is also obtained by $\mathbf{F} = \epsilon[-\frac{E|\mathbf{u}|}{\sqrt{Da}}\mathbf{u} - \frac{|\mathbf{u}|^{(n-1)}}{K^{*\prime}Da\sqrt{Gr}}\mathbf{u} + (T+NC)\mathbf{e_z}]$. The parameters of the mesoscopic method for the energy and concentration equation are calculated by $A_0 = T$; $\mathbf{B_i} = \frac{1}{2c^2}[\mathbf{u}T + \mathbf{q}]$ as the non-dimensional heat flux is implemented by $\mathbf{q} = -\frac{1}{Pr\,Gr^{\frac{1}{n+1}}}\nabla T$. In addition, $Z_0 = C$; $\mathbf{U_i} = \frac{1}{2c^2}[\mathbf{u}C - \frac{1}{Le\,Pr\,Gr^{\frac{1}{n+1}}}\nabla C]$. In this study, the applied mesh is $\Delta x = \Delta y = \Delta z = \frac{1}{60}$ and the selected time step is $\Delta t = 10^{-4}$. The Newtonian fluid ($n = 1$), shear thinning fluid ($0.3 \le n < 1$) and shear thickening fluid ($1 < n \le 1.4$) are evaluated. Figure 7 illustrates the isotherms, iscoconcentrations, and streamlines at $n = 0.8$, $Da = 10^{-3}$, $Gr = 10^3$, $Le = 1$, and $Pr = 100$ in the three dimensional double-diffusive natural convection of porous media for different porosities. It depicts that the gradient of the isotherms on the hot wall declines by the drop of the porosity. The pattern has been confirmed by the streamlines where the core of the streamlines demonstrates that the convection process weakens due to the decrease in porosity. The

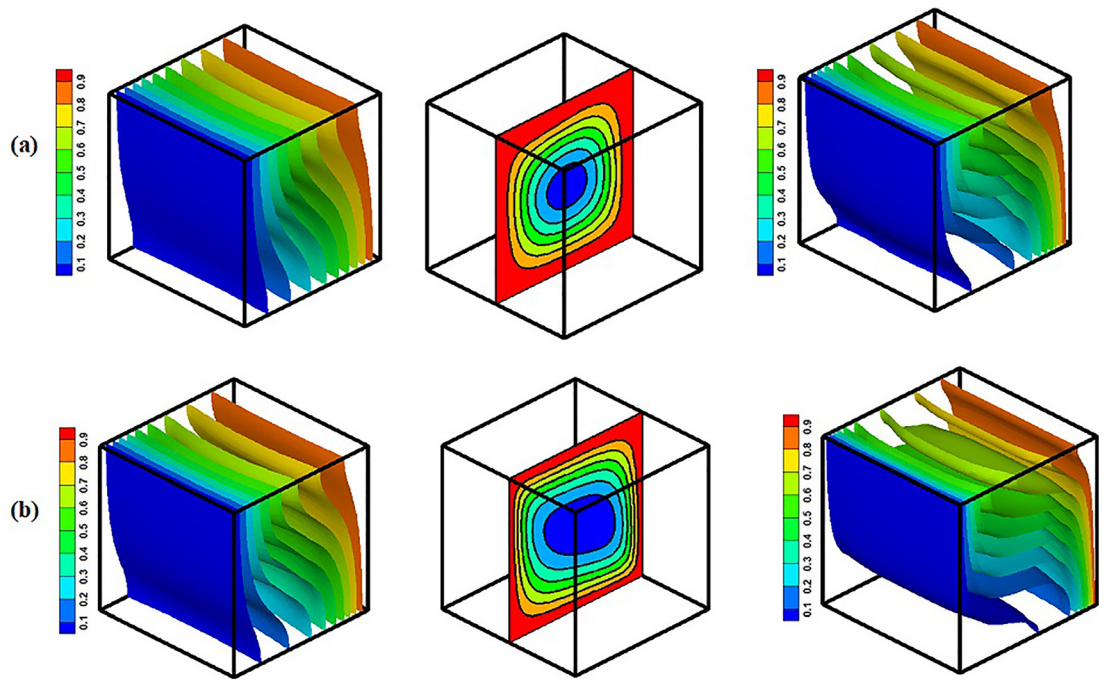

FIG. 7. Isotherms, streamlines, and isoconcentrations for different porosities (a) $\epsilon = 0.5$ and (b) $\epsilon = 0.9$ at $n = 0.8$, $Da = 10^{-3}$, $Gr = 10^3$, $Le = 1$, $N = 0.1$, and $Pr = 100$.

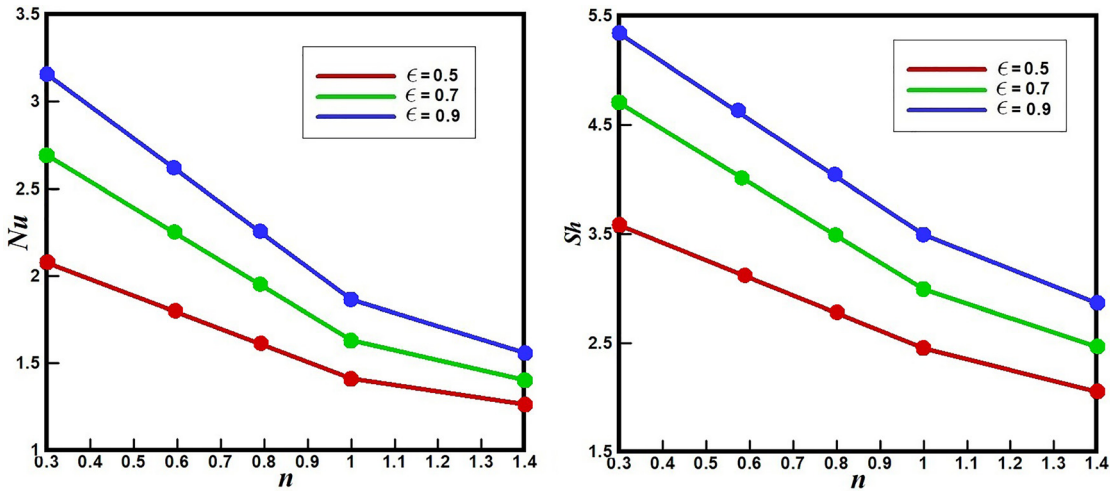

FIG. 8. The average Nusselt and Sherwood numbers for different power-law indexes (n) and porosities (ϵ) at $Gr = 10^3$, $Da = 10^{-3}$, $Le = 1$, $N = 0.1$, and $Pr = 100$.

average Nusselt and Sherwood numbers using Eqs. (62) and (63) are calculated and demonstrated for different power-law indexes and porosities at $Gr = 10^3$, $Da = 10^{-3}$, $Le = 1$, $N = 0.1$, and $Pr = 100$ in Fig. 8. It is clear that the average Nusselt and Sherwood numbers decline as the power-law index enhances. But, the porosity has a different effect on heat and mass transfer where the increase in the porosity augments the average Nusselt and Sherwood numbers significantly for the studied non-dimensional parameters. To assess the effect of Darcy number (which is directly proportional to the permeability of the porous medium) on heat and mass transfer in various power-law indexes, the average Nusselt and Sherwood numbers are calculated at $Gr = 10^3$, $\epsilon = 0.5$, $Le = 1$, $N = 0.1$, and $Pr = 100$ in Fig. 9. It shows that the average Nusselt and Sherwood numbers in various porosities decrease due to the drop of the Darcy number in all studied power-law indexes. In addition, it reveals that the rise of power-law index from $n = 0.3$ to 1.4 declines heat and mass transfer gradually. However, it demonstrates that the effect of the power-law index is marginal at $Da = 10^{-4}$ compared to higher values of Darcy numbers. The pattern also is observed by the data plotted in Fig. 10 which demonstrates that the magnitudes of the velocity and temperature components in the middle of the cubic cavity enhance significantly with increasing Darcy number when other parameters are kept unaltered. In fact, the rise of Darcy number causes the drag force due to porous media in the momentum equation to become smaller compared to the strength of the buoyancy force. So, the effects of convection become increasingly strong.

IV. CONCLUSION

In the present work, a comprehensive numerical method, using LBM for two- and three-dimensional cases, is presented which can derive the macroscopic equations of continuity, momentum, energy, and concentration for laminar incompressible flows of power-law

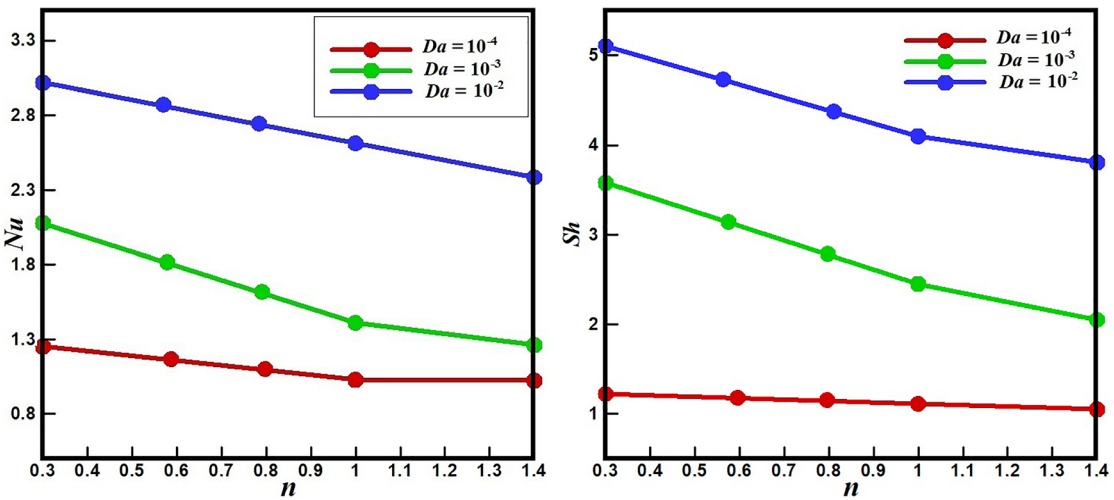

FIG. 9. The average Nusselt and Sherwood numbers for different power-law indexes (n) and Darcy numbers (Da) at $Gr = 10^3$, $\epsilon = 0.5$, $Le = 1$, $N = 0.1$, and $Pr = 100$.

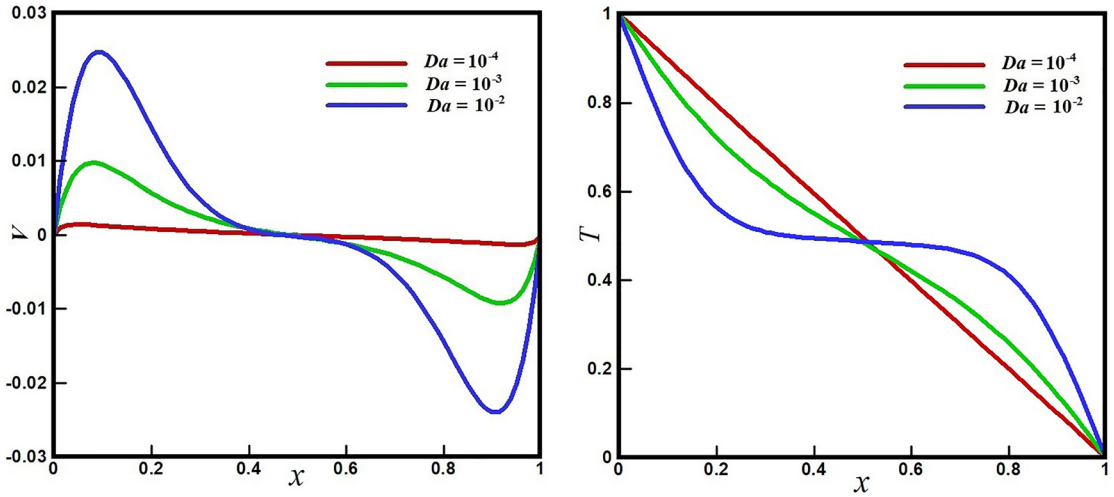

FIG. 10. The velocity and temperature distributions in the x direction at $y = z = 0.5$ for various Darcy numbers at $Gr = 10^3$, $\epsilon = 0.5$, $n = 0.8$, $Le = 1$, $N = 0.1$, and $Pr = 100$.

fluids in porous media. The proposed method can be utilized to solve isothermal, thermal, and solutal problems of non-Newtonian power-law fluids in porous media without applying any assumptions and covering all terms in the mentioned equations. In addition, it is possible to apply various REV approaches for the porous media in this method, e.g., Darcy, Forchheimer–Darcy, Darcy–Brinkman, and the general Darcy–Forchheimer–Brinkman models. In contrast to the conventional LBM for porous media,[64,65] which applied a force term due to the porosity in the distribution function, an equilibrium distribution function based on macroscopic variables of the momentum equation for the applied porous model is derived. Different from conventional LBM, which utilizes specific distribution function relations for boundary conditions, various macroscopic boundary conditions of velocity, temperature, and concentration can be imposed directly in different Neumann and Dirichlet boundary conditions. The introduced method was validated by previous studies and the good agreement between them demonstrated the accuracy of this approach. It was shown that the present method can be applied effectively for thermal–solutal problems of non-Newtonian power-law fluids through porous media where double-diffusive natural convection of power-law fluids in a porous enclosure for two- and three-dimensional cases was simulated and presented for different non-dimensional parameters.

The present mesoscopic method only considered REV models with the assumption of the local thermal equilibrium (LTE) between fluid and solid phases. In our future studies, the present approach will be developed for local thermal non-equilibrium (LTNE) in porous media.

NOMENCLATURE

$\mathbf{a}$	Acceleration
$\mathbf{A_1}$	First Rivlin–Ericksen tensor
c	Lattice speed
c_p	Specific heat capacity at constant pressure
C	concentration
C_t	Tortuosity factor
d	Diameter of solid particle
D	Mass diffusivity
Da	Darcy number
D_{CT}	Dufour coefficient
D_{TC}	Soret coefficient
$\mathbf{e}$	Particle speed
$\mathbf{e}_y$	Unit vector in y direction
$\mathbf{e}_z$	Unit vector in z direction
E	Inertial coefficient
Ec	Eckert number
f	Density distribution functions
f^{eq}	Equilibrium density distribution functions
F	Total body force
$\mathbf{F}$	External forces
g	Internal energy distribution functions
$\mathbf{g}$	Gravity acceleration
g^{eq}	Equilibrium internal energy distribution functions
G	Gain component
h	Internal concentration distribution functions
h_α^{eq}	Equilibrium internal concentration distribution functions
H	Height of the cavity
$\mathbf{J}$	total mass flux
k	Thermal conductivity
K	Permeability
K^*	Modified permeability
L	Length of the cavity
Le	Lewis number
n	Power-law index
N	Buoyancy ratio
Nu	Average Nusselt number
p	Pressure
Pr	Prandtl number
$\mathbf{q}$	Heat flux
$\mathbf{q}'$	Heat flux due to the concentration gradient

R	Ideal gas
Ra	Rayleigh number
Sh	Average Sherwood number
t	Time
T	Temperature
u	Velocity in x direction
U	The buoyancy velocity scale
v	Velocity in y direction
w	Velocity in z direction
x, y, z	Cartesian coordinates

Greek letters

α	Thermal diffusivity
β_C	Solutal expansion coefficient
β_T	Thermal expansion coefficient
$\dot{\gamma}$	Shear rate
Δt	Time increment
Δx	Lattice spacing in x direction
Δy	Lattice spacing in y direction
Δz	Lattice spacing in z direction
ϵ	Porosity
λ	Non-dimensional relaxation time
μ	Dynamic viscosity
Ξ	Internal energy density
ρ	Density of fluid
σ	Differential collision cross section
$\boldsymbol{\tau}$	Extra stress tensor
Υ	Collision operator
ϕ	Relaxation time
Φ	Viscous dissipation
ω	Weighting factor
ϖ	Dimensional relaxation time

Subscripts

a	Advective
avg	Average
C	Cold
d	Diffusive
e	Effective
f	Fluid
H	Hot
i	SPECIFIC node
L	Left
m	Mean
r	Relative
R	Right
s	Solid
0	Initial

APPENDIX A: REV MODELS FOR NEWTONIAN FLUIDS

The first and foremost REV model which has been utilized widely in multifarious subjects and disciplines is the Darcy model. In this approach, it is assumed that a Newtonian fluid passes through an isotropic porous medium while the flow is laminar and steady. The proposed mathematical model of the Darcy model for the momentum equation is written as

$$\frac{\mu}{K}\mathbf{u} = -\nabla p, \tag{A1}$$

where $\mathbf{u}$, K, and p are the velocity, the permeability of the porous medium, and pressure; respectively. The continuity equation for the case of incompressible flow is expressed by $\nabla \cdot \mathbf{u} = 0$. However, the Darcy model can be accurate in intense flows, high porosity materials, and near the boundaries due to the negligence of the inertia term. To evaluate the inertia term, various methods were introduced and one common idea is to adopt the Forchheimer–Darcy equation,[5,6] which can be stated as

$$\frac{\mu}{K}\mathbf{u} + \frac{\rho E}{\sqrt{K}}\mathbf{u}|\mathbf{u}| = -\nabla p, \tag{A2}$$

where ρ is the density and E is the inertia coefficient (or the Forchheimer correction factor), as it plays the role of porous inertia effects (i.e., separation and wake effects) which are relevant at higher flow velocities. The Forchheimer correction factor which is an empirical factor and can be defined by a relation with porosity (ϵ), e.g., $E = \frac{a}{\sqrt{a'\epsilon^3}}$ and the parameters of a and a' are constants which were defined in various previous theoretical and empirical studies. When $E = 0$, i.e., when Forchheimer effects can be neglected, the model reduces to the conventional Darcy law. Brinkman[7] noted that the Darcy model can be useful for small permeabilities, but not for higher ones. Another drawback of the Darcy model is the difficulty in defining and framing boundary conditions in porous parts and adjoining empty space. To tackle this issue, Brinkman suggested adding the effects of the viscous shearing stresses to consider the influences and formulate rational boundary conditions. So, the proposed equation was the combination of pressure gradient, the divergence of the viscous stress tensor, and the damping force due to the porous mass as follows:

$$\frac{\mu}{K}\mathbf{u} = -\nabla p + \mu_e \nabla^2 \mathbf{u}, \tag{A3}$$

where μ_e represents the effective viscosity of the fluid (called as a factor by Brinkman). The main advantage of the Brinkman model is that it is a reduced form of the Navier–Stokes equation for high permeability cases and approaches to an asymptote of the Darcy equation for low permeability. Some researchers have considered the effective dynamic viscosity equals to the dynamic viscosity ($\mu_e = \mu$) for weak flow in porous media. But, many other relations for the effective dynamic viscosity were suggested in the Brinkman's model since it has shown in various numerical simulations that the effective viscosity is smaller or larger than the viscosity. For example, Ochoa-Tapia and Whitaker[8] showed that μ_e is identical to μ/ϵ. Lundgren[9] found $\mu_e < \mu$ when the porosity is smaller than 0.7 ($\epsilon < 0.7$). It was also shown that the Brinkman equation is appropriate for $\epsilon > 0.8$ by the study of Rubinstein[10] and $\epsilon > 0.95$ by the work of Durlofsky and Brady.[11] So, the Brinkman model demonstrates better results with increasing the value of porosity.

Vafai and Tien[12] applied the two elements of inertial forces and solid boundary simultaneously by the volume-averaging technique and introduced the governing equation of momentum for isotropic medium and incompressible flow as[13]

$$\frac{\rho}{\epsilon^2}(\mathbf{u}\cdot\nabla\mathbf{u}) = -\nabla p + \frac{\mu}{\epsilon}\nabla^2\mathbf{u} - \frac{\mu}{K}\mathbf{u} - \frac{\rho E}{\sqrt{K}}\mathbf{u}|\mathbf{u}|. \quad \text{(A4)}$$

The concept of the volume-averaging was introduced by Whitaker[14–16] who applied the technique to study porous media with deriving the Darcy law by the integration of the Navier–Stokes equation. Vafai and Kim[17] indicated that the momentum formulation in Eq. (A4) had shown an excellent agreement with experimental results. In addition, it is significantly important for analyzing fluids in regions with partially porous media. The parameters of K and E in this model were calculated by Vafai[18] in the form of $K = \frac{\epsilon^3 d^2}{150(1-\epsilon)^2}$, and $E = \frac{1.75}{\sqrt{150\,\epsilon^3}}$ where d is the diameter of the solid particle.

Lauriat and Prasad[19] studied the unsteady Brinkman-extended Darcy model including the transport and viscous terms for natural convection in vertical porous cavities. Assuming that the solid particles and the fluid are in thermal equilibrium, they derived the momentum equation in the absence of the gravity force as

$$\frac{\rho}{\epsilon}\frac{\partial\mathbf{u}}{\partial t} + \frac{\rho}{\epsilon^2}(\mathbf{u}\cdot\nabla)\mathbf{u} = -\nabla p + \mu_e\nabla^2\mathbf{u} - \frac{\mu}{K}\mathbf{u}. \quad \text{(A5)}$$

The generalized form of the momentum, energy, and concentration balance equations based on the Brinkman–Forchheimer extended Darcy model for unsteady flow was modified and given as[1–4,20–25]

$$\frac{\rho}{\epsilon}\left[\frac{\partial\mathbf{u}}{\partial t} + (\mathbf{u}\cdot\nabla)\frac{\mathbf{u}}{\epsilon}\right] = -\nabla p + \frac{\mu}{\epsilon}\nabla^2\mathbf{u} - \frac{\mu}{K}\mathbf{u} - \frac{\rho E}{\sqrt{K}}\mathbf{u}|\mathbf{u}|, \quad \text{(A6)}$$

$$\sigma\frac{\partial T}{\partial t} + \mathbf{u}.\nabla T = \alpha_e\nabla^2 T + D_{TC}\nabla^2 C + \Phi, \quad \text{(A7)}$$

$$\epsilon\frac{\partial C}{\partial t} + \mathbf{u}.\nabla C = D_e\nabla^2 C + D_{CT}\nabla^2 T, \quad \text{(A8)}$$

where T is temperature and α_e is the effective thermal diffusivity, which is calculated by $\alpha_e = k_e/(\rho c_p)_f$. σ is defined by $\sigma = \frac{(\rho c_p)_e}{(\rho c_p)_f}$. Here, k_e is the effective thermal conductivity and calculated by $k_e = k_f + (1-\epsilon)k_s$ where the subscripts of f and s refer to the fluid and solid phases; respectively. c_p is the heat capacity of the fluid. In addition, $(\rho c_p)_e$ is found by $(\rho c_p)_e = \epsilon(\rho c_p)_f + (1-\epsilon)(\rho c_p)_s$. Φ is the viscous dissipation and calculated by[23–25]

$$\Phi = \left[\frac{\mu}{K}\mathbf{u} + \frac{\rho E}{\sqrt{K}}\mathbf{u}|\mathbf{u}|\right]\cdot\mathbf{u} + \frac{1}{2}\mu_e(\mathbf{A}_1 : \mathbf{A}_1), \quad \text{(A9)}$$

where $\mathbf{A}_1$ is the first Rivlin Ericksen tensor and defined by $\mathbf{A}_1 = \nabla\mathbf{u} + (\nabla\mathbf{u})^T$. C is the concentration and D_e is the effective mass diffusivity coefficient. Here, D_{TC} and D_{CT} are the Soret and Dufour coefficients, respectively. It should be mentioned that the viscous dissipation and the Dufour parameter in the energy equation and the Soret parameter in the concentration equation can be neglected in most cases.

APPENDIX B: CONVENTIONAL LATTICE BOLTZMANN METHOD (LBM)

The single particle distribution function $[f = f(\mathbf{x}, \mathbf{e}, t)]$ is the key variable in kinetic theory which represents the number of molecules (particles) with the unit mass $m = 1$, velocity $\mathbf{e}$ at position $\mathbf{x}$ and time t which has the following relationship with the macroscopic density

$$\rho = \int f\, d\mathbf{e}. \quad \text{(B1)}$$

In addition, the macroscopic velocity $\mathbf{u}$ and temperature T can be obtained by the momentum density and the internal energy density, respectively, as follows:

$$\rho\mathbf{u} = \int \mathbf{e}f\, d\mathbf{e} = 0\,, \quad \rho\Xi = \frac{1}{2}\int v_r^2 f\, d\mathbf{e} = 0, \quad \text{(B2)}$$

where Ξ is the internal energy density and calculated by $\Xi = \frac{D_0}{2}RT$ with D_0 being the number of degrees of freedom of a particle and R is the ideal gas constant. Moreover, v_r is the magnitude of the relative velocity; which is the difference between the particle velocity and the local mean velocity and defined by $v_r = |\mathbf{e} - \mathbf{u}|$. The rate of change of the distribution function of particles before and after a collision can be defined by a collision operator $[\Upsilon(f)]$ as

$$\frac{df}{dt} = \Upsilon(f). \quad \text{(B3)}$$

The collision operator $\Upsilon(f)$ satisfies the conservation of mass, momentum, and the total energy conservation. Based on the definition of the distribution function f and its functions, its total derivative is found as

$$\frac{df}{dt} = \frac{\partial f}{\partial\mathbf{x}}\frac{d\mathbf{x}}{dt} + \frac{\partial f}{\partial\mathbf{e}}\frac{d\mathbf{e}}{dt} + \frac{\partial f}{\partial t}\frac{dt}{dt}. \quad \text{(B4)}$$

So, Eq. (B4) can be written as

$$\frac{df}{dt} = \frac{\partial f}{\partial\mathbf{x}}\mathbf{e} + \frac{\partial f}{\partial\mathbf{e}}\mathbf{a} + \frac{\partial f}{\partial t}. \quad \text{(B5)}$$

Here, $\mathbf{a}$ is the acceleration of the particles and based on the second Newtonian's law $\mathbf{a} = \mathbf{F}/m$ with $\mathbf{F}$ being the intermolecular and external forces. The collision part $\Upsilon(f)$ is the difference between the Gain (G) and Loss (L) components of the two-particle collision and is presented by an integral equation as

$$\Upsilon(f) = G - L = \int (f_1' f_2' - f_1 f_2)\, v_r\sigma(\Omega, v_r)\, d\Omega\, d\mathbf{v}_2, \quad \text{(B6)}$$

where f_1', f_2' are the distribution functions of the two particles after collisions. $\sigma(\Omega, v_r)$ is the differential collision cross section for the two particles during the collision process which has the velocities of $\mathbf{u}_1, \mathbf{u}_2$ (incoming, before the collision) into $\mathbf{u}_1', \mathbf{u}_2'$ (outgoing, after collision).

Finally, the classic continuum Boltzmann equation for one particle with the unit mass and consideration to Eqs. (B1)–(B6) is written in the form of an integrodifferential equation as

$$\frac{\partial f}{\partial t} + \mathbf{e}\cdot\nabla_{\mathbf{x}} f + \mathbf{F}\cdot\nabla_{\mathbf{e}} f = \int (f_1' f_2' - f_1 f_2)\, v_r\sigma(\Omega, v_r)\, d\Omega\, d\mathbf{v}_2. \quad \text{(B7)}$$

The complicated integral in the collision part in the RHS of Eq. (B7) encouraged researchers to introduce a simplified approximation for the presented integral in the collision and the most well-

known one is the Bhatnagar–Gross–Krook (BGK) collision approximation (Υ_B), which is defined as

$$\Upsilon_B = \frac{-1}{\varpi_f}(f - f^{eq}). \tag{B8}$$

Then, the lattice Boltzmann–BGK (LBGK) equation with considering the force term can be written as

$$\frac{\partial f}{\partial t} + \mathbf{e}\cdot\nabla_{\mathbf{x}} f + \mathbf{F}\cdot\nabla_{\mathbf{e}} f = \frac{-1}{\varpi_f}(f - f^{eq}), \tag{B9}$$

where ϖ_f is the dimensional relaxation time due to collision and f^{eq} is the equilibrium distribution functions, which is found in conventional LBM as

$$f^{eq} \equiv f^{eq}(\rho, \mathbf{u}, T, \mathbf{e}) = \frac{\rho}{(2\pi RT)^{D_0/2}} \exp\left[-\frac{(\mathbf{e}-\mathbf{u})^2}{2RT}\right]. \tag{B10}$$

To find the third term in Eq. (B9) in the presence of the force term, considering the equation for f^{eq} in Eq. (B10) is assumed as

$$\nabla_{\mathbf{e}} f \approx \nabla_{\mathbf{e}} f^{eq} = -\frac{(\mathbf{e}-\mathbf{u})}{RT} f^{eq}. \tag{B11}$$

The exponential function in Eq. (B10) can be expanded by a Taylor series and approximated as

$$f^{eq} = \rho\omega\left[1 + \frac{\mathbf{e}\cdot\mathbf{u}}{c_s^2} + \frac{(\mathbf{e}\cdot\mathbf{u})^2}{2c_s^4} - \frac{|\mathbf{u}|^2}{2c_s^2}\right], \tag{B12}$$

where $\omega = \exp\left(-\frac{\mathbf{e}.\mathbf{e}}{2RT}\right)(2\pi RT)^{-D_0/2}$ and $c_s = \sqrt{RT}$, which is the speed of sound. Now, Eq. (B9) can be revised as

$$\frac{\partial f}{\partial t} + \mathbf{e}\cdot\nabla_{\mathbf{x}} f = \frac{-1}{\varpi_f}(f - f^{eq}) + \mathbf{F}\cdot\frac{(\mathbf{e}-\mathbf{u})}{RT} f^{eq}. \tag{B13}$$

A discretized form of Eq. (B13) can be written as

$$\frac{\partial f_i}{\partial t} + \mathbf{e_i}\cdot\nabla_{\mathbf{x}} f_i = \frac{-1}{\varpi_f}\left(f_i - f_i^{eq}\right) + F_i, \tag{B14}$$

where $F_i = \mathbf{F}\cdot\frac{(\mathbf{e_i}-\mathbf{u})}{RT} f_i^{eq}$. Next, integrating Eq. (B14) over a time interval Δt with e^t/ϖ_f as the integrating factor and linearizing in terms of this time interval, Eq. (B13) is changed to

$$\begin{aligned} &f_i(\mathbf{x} + \mathbf{e_i}\Delta x, t + \Delta t) - f_i(\mathbf{x}, t) \\ &\quad = -\frac{1}{\lambda_f}\left[f_i(\mathbf{x}, t) - f_i^{eq}(\mathbf{x}, t)\right] + F_i(\mathbf{x}, t)\,\Delta t, \end{aligned} \tag{B15}$$

where $\lambda_f = \varpi_f/\Delta t$ is the non-dimensional relaxation time and the discretized equilibrium distribution functions and the force term $F_i(\mathbf{x}, t)$ are derived as

$$f_i^{eq} = \rho\omega_i\left[1 + \frac{\mathbf{e_i}\cdot\mathbf{u}}{c_s^2} + \frac{(\mathbf{e_i}\cdot\mathbf{u})^2}{2c_s^4} - \frac{|\mathbf{u}|^2}{2c_s^2}\right], \tag{B16}$$

$$F_i(\mathbf{x}, t) = \omega_i\rho\left(1 - \frac{1}{2\lambda_f}\right)\left[\frac{\mathbf{e_i}\cdot\mathbf{F}}{c_s^2} + \frac{\mathbf{uF} : (\mathbf{e_i}\mathbf{e_i} - c_s^2\mathbf{I})}{c_s^4}\right]. \tag{B17}$$

For applying the method and discretized equations, a specific lattice should be defined. So, the parameter of DmQn is used where m presents the dimension of the study (2D or 3D) and n is the number of nodes in the selected lattice. For example, in the D2Q9 model, there are nine discrete velocities in the lattice $i = 0, 1, \ldots, 8$ for a two-dimensional case (Fig. 11) and are defined by[59]

$$\mathbf{e_i} = \begin{cases} (0,0), & i = 0 \\ c(\cos\theta_i, \sin\theta_i), & i = 1,3,5,7 \\ c\sqrt{2}(\cos\theta_i, \sin\theta_i), & i = 2,4,6,8, \end{cases} \tag{B18}$$

where θ_i is calculated by $\theta_i = (\alpha - 1)\pi/4$. In the D3Q15 model, there are fifteen discrete velocities for a three-dimensional case in the lattice (Fig. 12): $i = 0, 1, \ldots, 14$ and are given by

$$\mathbf{e_i} = \begin{cases} 0, & i = 0 \\ c(\pm 1, 0, 0), c(0, \pm 1, 0), c(0, 0, \pm 1), & i = 1 - 6 \\ c(\pm 1, \pm 1, \pm 1), & i = 7 - 14, \end{cases} \tag{B19}$$

where $c = \Delta x/\Delta t$ and Δx is the lattice spacing. The macroscopic density and velocity are found as

$$\rho = \sum_{i=0}^{M} f_i, \quad \rho\mathbf{u} = \sum_{i=0}^{M} f_i\mathbf{e_i}, \tag{B20}$$

where ω_i is the weighting factor which can be defined by mass and momentum conservation, as well as isotropy. It is determined for D2Q9 by $\omega_0 = 4/9$; $\omega_i = 1/9$, $i = 1,3,5,7$; $\omega_i = 1/36$, $i = 2,4,6,8$ and for D3Q15 it is equal to $\omega_0 = 2/9$; $\omega_i = 1/9$, $i = 1-6$; $\omega_i = 1/72$, $i = 7-14$. c_s is defined by $c_s = c/\sqrt{3}$. The effective kinematic viscosity is determined by $\nu = c_s^2(\lambda_f - 0.5)\Delta t$ and the pressure (p) is found by $p = c_s^2\rho$. The LBE of temperature distribution function for finding temperature and satisfying the energy equation is given as

$$\frac{\partial g_i}{\partial t} + \mathbf{e_i}\cdot\nabla_{\mathbf{x}} g_i = \frac{-1}{\varpi_g}\left(g_i - g_i^{eq}\right), \tag{B21}$$

where ϖ_g is the relaxation time. The discretized form of Eq. (B21) can be written as

$$g_i(\mathbf{x} + \mathbf{e_i}\Delta x, t + \Delta t) - g_i(\mathbf{x}, t) = -\frac{1}{\lambda_g}\left[g_i(\mathbf{x}, t) - g_i^{eq}(\mathbf{x}, t)\right], \tag{B22}$$

where g_i is the temperature distribution function, λ_g is the dimensionless relaxation time for the temperature and is defined by

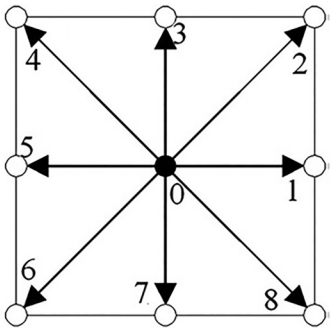

FIG. 11. Discrete velocity distribution in D2Q9.

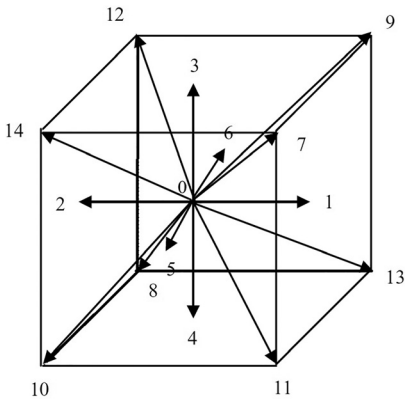

FIG. 12. Discrete velocity distribution in D3Q15.

$\frac{1}{c_s^2\Delta t}\alpha + 0.5 = \lambda_g$ where α is the thermal diffusivity. The equilibrium temperature distribution function g_i^{eq} is found by

$$g_i^{eq}(\mathbf{x},t) = \omega_i T\left[1 + \frac{\mathbf{e_i}\cdot\mathbf{u}}{c_s^2}\right] \tag{B23}$$

and the fluid temperature T is defined by

$$T = \sum_{i=0}^{M} g_i. \tag{B24}$$

Different models for advection-diffusion equations were proposed in LBM[60–62] and a general method for concentration equations which satisfies the concentration equations is as[63]

$$\frac{\partial h_i}{\partial t} + \mathbf{e_i}\cdot\nabla_{\mathbf{x}} h_i = \frac{-1}{\varpi_h}\left(h_i - h_i^{eq}\right), \tag{B25}$$

where ϖ_h is the relaxation time. The discretized form of Eq. (B25) can be written as

$$h_i(\mathbf{x} + \mathbf{e_i}\Delta x, t + \Delta t) - h_i(\mathbf{x},t) = -\frac{1}{\lambda_h}\left[h_i(\mathbf{x},t) - h_i^{eq}(\mathbf{x},t)\right], \tag{B26}$$

while the equilibrium temperature distribution is proposed similar the approach of fluid flow and temperature field as

$$h_i^{eq}(\mathbf{x},t) = \omega_i C\left[1 + \frac{\mathbf{e_i}\cdot\mathbf{u}}{c_s^2}\right], \tag{B27}$$

where h_i is the concentration distribution function, λ_h is the dimensionless relaxation time for concentration and is defined by $\frac{1}{c_s^2\Delta t}D + 0.5 = \lambda_h$ where D is the mass diffusivity coefficient. Then, the concentration can be calculated by

$$C = \sum_{i=0}^{M} h_i. \tag{B28}$$

The most popular model for studying porous media with REV is the proposed model by Guo and Zhao[64] that introduced for isothermal incompressible Newtonian fluid flow in porous media. They considered the generalized model for porous media and recovered Eq. (A6) from the proposed model. The total body force $F_i(\mathbf{x},t)$ in the RHS of Eq. (B15) is the summation of the force due to the presence of the porous medium and other external forces ($\mathbf{F}'$), which is given by

$$F_i(\mathbf{x},t) = \omega_i\rho\left(1 - \frac{1}{2\lambda_f}\right)\left[\frac{\mathbf{e_i}\cdot\mathbf{F}}{c_s^2} + \frac{\mathbf{uF}:(\mathbf{e_i}\mathbf{e_i} - c_s^2\mathbf{I})}{\epsilon c_s^4}\right], \tag{B29}$$

$$\mathbf{F} = -\frac{\epsilon\mu}{K}\mathbf{u} - \frac{\rho\,\epsilon\,E}{\sqrt{K}}\mathbf{u}|\mathbf{u}| + \epsilon\mathbf{F}'. \tag{B30}$$

They also modified the equilibrium distribution function for porous media as

$$f_i^{eq}(\mathbf{x},t) = \omega_i\rho\left[1 + \frac{\mathbf{e_i}\cdot\mathbf{u}}{c_s^2} + \frac{(\mathbf{e_i}\cdot\mathbf{u})^2 - c_s^2|\mathbf{u}|^2}{2\epsilon c_s^4}\right]. \tag{B31}$$

Guo and Zhao[65] developed the model for thermal problems and applied for studying natural convection in a porous cavity. The used LBE of temperature distribution function and the equilibrium temperature distribution function are similar to Eqs. (B22) and (B23) since the modified velocity due to porous media is imposed in the equations. But, the temperature has the following relation with the temperature distribution function

$$\frac{(\rho c_p)_e}{(\rho c_p)_f}T = \sum_{i=0}^{M} g_i, \tag{B32}$$

where the dimensionless relaxation time for the temperature in porous media was given by $\frac{1}{c_s^2\Delta t}\alpha_m + 0.5 = \lambda_g$. However, it was proposed by some researchers[66–69] the equilibrium temperature distribution function should also be modified similar to the fluid flow part [e.g., with dividing the second term of LHS of Eq. (B23) to porosity (ϵ)]. There are limited studies into the thermal–solutal process through porous media by LBM while the fluid is considered as Newtonian. In most cases, the method of Guo[64,65] was used for the concentration part. However, Chen *et al.*[70] noted that the model has a significant issue that the porosity in the studied domain should be uniform. Further, the effective mass diffusivity depends on the porosity which is nonphysical. So, they proposed a new concentration equation while applied the same fluid flow and temperature LBEs of Guo's model.

In the past two decades, LBM has been used for studying isothermal and thermal problems of Newtonian and non-Newtonian fluids through porous media.[71–77] For studying non-Newtonian fluids, in the conventional LBM the non-dimensional relaxation time is locally altered as a function of the shear-rate $\dot{\gamma}$ since the dynamic viscosity is not constant and is changing. So, we have

$$\lambda(\mathbf{x},t) = \frac{1}{c_s^2\Delta t}\left(\frac{\eta(\mathbf{x},t)}{\rho(\mathbf{x},t)}\right) + 0.5. \tag{B33}$$

In this approach, the first Rivlin Ericksen $\mathbf{A}_1$ for a two-dimensional case was found to be

$$\mathbf{A}_1 = \frac{1}{\lambda(\mathbf{x},t)c_s^2\rho\Delta t}\sum_{i=0}^{M}\mathbf{e_i}\mathbf{e_i}\left[f_i(\mathbf{x},t) - f_i^{eq}(\mathbf{x},t)\right]. \tag{B34}$$

It is clear that the variation of the local shear rate is directly related to the relaxation time which would not be avoidable to face numerical instability. In addition, the relation restricts the model and cannot deal with a wide range of non-Newtonian fluid models.

Furthermore, in all of the mentioned studies, the terms of viscous dissipation, Soret and Dufour parameters were neglected and the terms were not derived.

The viscous dissipation in uniform Newtonian fluid flow was investigated using LBM in some previous studies. He *et al.*[78] proposed an LBM for studying thermo-hydrodynamics in incompressible flows. The model had the advantage to consider the viscous dissipation and compression work due to pressure. The approach was assessed by simulating two benchmarks of Couette flow and Rayleigh–Benard convection. In this method, the effect of the viscous dissipation in the internal distribution energy equation was improved by adding a source term in the LHS of Eq. (B22) as follows:

$$g_i(\mathbf{x}+\mathbf{e_i}\Delta x, t+\Delta t) - g_i(\mathbf{x},t) = -\frac{1}{\lambda_g}\left\{\left[g_i(\mathbf{x},t) - g_i^{eq}(\mathbf{x},t)\right] + f_i(\mathbf{x},t)q_i(\mathbf{x},t)\Delta t\right\}, \tag{B35}$$

$$q_i(\mathbf{x},t) = (\mathbf{e_i}-\mathbf{u})\cdot\left[\frac{1}{\rho}(-\nabla p + \nabla.\boldsymbol{\tau}) + (\mathbf{e_i}-\mathbf{u}).\nabla\mathbf{u}\right]. \tag{B36}$$

Shi *et al.*[79] simplified the model of He *et al.*[78] based on a LBGK equation for thermal flows with studying the viscous dissipation in incompressible flow. They evaluated and validated the proposed method by simulating laminar incompressible convection with and without heat dissipation in Couette and Poiseuille flow. Finally, they recovered the macroscopic equations through Chapman–Enskog procedure. They added a source term to the LHS of the internal distribution energy equation (B22) for small Mach number as

$$g_i(\mathbf{x}+\mathbf{e_i}\Delta x, t+\Delta t) - g_i(\mathbf{x},t) = -\frac{1}{\lambda_g}\left[g_i(\mathbf{x},t) - g_i^{eq}(\mathbf{x},t)\right] + \Delta t R', \tag{B37}$$

$$R' = -2/3R\left[f_i(\mathbf{x},t) - f_i^{eq}(\mathbf{x},t)\right](\mathbf{e_i}-\mathbf{u})(\mathbf{e_i}-\mathbf{u}) : \frac{\partial \mathbf{u}}{\partial \mathbf{x}}. \tag{B38}$$

It should be noted that the viscous dissipation had a significant effect in the uniform Newtonian fluid when the flows have high Prandtl number ($Pr = \frac{\mu}{\rho\alpha}$) and Eckert number ($Ec = \frac{u^2}{c_p\Delta T}$) since the compression work in the compressible flow is neglected.

The boundary conditions in conventional LBM are imposed by the relation between the distribution functions and/or equilibrium distribution functions. For example, the bounce-back approach is used for no-slip boundary conditions, which assumes that the particles hitting the boundary reflect back. Another approach which is suitable for Dirichlet boundary conditions is the non-equilibrium extrapolation, which decomposes the distribution function at the boundary node into its equilibrium and non-equilibrium parts.

APPENDIX C: THE DISCRETE PARTICLE DISTRIBUTION FUNCTION

Recalling the LBGK equation (B14), we have

$$\frac{\partial f_i}{\partial t} + \mathbf{e_i}\cdot\nabla_{\mathbf{x}} f_i = \frac{-1}{\varpi_f}\left(f_i - f_i^{eq}\right) + F_i. \tag{C1}$$

To have the introduced f_i^{eq} in the equation, the following conditions should be satisfied.

$$\sum_{i=0}^{8} f_i^{eq} = \rho, \tag{C2}$$

$$\sum_{i=0}^{8} f_i^{eq}\mathbf{e}_i = \rho\mathbf{u}, \quad \mathbf{u} = u\mathbf{i} + v\mathbf{j}, \tag{C3}$$

$$\sum_{i=0}^{8} f_i^{eq}\mathbf{e}_i \otimes \mathbf{e}_i = \mathbf{M}, \tag{C4}$$

where

$$\mathbf{M} = \begin{bmatrix} \mathrm{M}_{xx} & \mathrm{M}_{xy} \\ \mathrm{M}_{yx} & \mathrm{M}_{yy} \end{bmatrix}, \tag{C5a}$$

$$\mathrm{M}_{xx} = \rho\frac{u^2}{\epsilon} + \epsilon p - \frac{1}{\epsilon^{(n-1)}}\tau_{xx}, \tag{C5b}$$

$$\mathrm{M}_{xy} = \mathrm{M}_{yx} = \rho\frac{uv}{\epsilon} - \frac{1}{\epsilon^{(n-1)}}\tau_{xy}, \tag{C5c}$$

$$\mathrm{M}_{yy} = \rho\frac{v^2}{\epsilon} + \epsilon p - \frac{1}{\epsilon^{(n-1)}}\tau_{yy}. \tag{C5d}$$

Further, the following conditions for the proposed force term in the equation should be satisfied:

$$\sum_{i=0}^{8} F_i = 0\,, \quad \sum_{i=0}^{8} F_i\mathbf{e}_i = \mathbf{F}. \tag{C6}$$

The Chapman–Enskog expansion is used for f_i as

$$f_i = f_i^{eq} + \zeta f_i^{(1)} + \zeta^2 f_i^{(2)} + O(\zeta^3). \tag{C7}$$

Now, substituting the f_i in (C7) into (C1), we find that

$$\frac{\partial f_i^{eq}}{\partial t} + \nabla\cdot(f_i^{eq}\mathbf{e}_i) - F_i = -\frac{1}{\varpi_f}f_i^{(1)} + O(\varepsilon). \tag{C8}$$

Summing the equation above, we obtain

$$\frac{\partial}{\partial t}\left(\sum_{i=0}^{8} f_i^{eq}\right) + \nabla\cdot\left(\sum_{i=0}^{8} f_i^{eq}\mathbf{e}_i\right) + \left(\sum_{i=0}^{8} F_i\right) = -\frac{1}{\varpi_f}\sum_{i=0}^{8} f_i^{(1)} + O(\varepsilon). \tag{C9}$$

Using Eq. (C2), (C3), and (C6) and considering ρ as a constant for an incompressible flow, Eq. (C9) reduces to

$$\rho(\nabla\cdot\mathbf{u}) = 0 + O(\varepsilon). \tag{C10}$$

Actually, (C10) is the continuity equation of an incompressible medium and show the proposed method satisfies the continuity equation. Multiplying (C9) by $\mathbf{e}_i$,

$$\frac{\partial f_i^{eq}\mathbf{e}_i}{\partial t} + (\mathbf{e}_i\cdot\nabla_{\mathbf{x}} f_i^{eq})\mathbf{e}_i - F_i\mathbf{e}_i = -\frac{1}{\varpi_f}\mathbf{e}_i f_i^{(1)} + O(\varepsilon), \tag{C11}$$

we also have

$$\nabla\cdot(f_i^{eq}\mathbf{e}_i\otimes\mathbf{e}_i) = (\mathbf{e}_i\cdot\nabla_{\mathbf{x}} f_i^{eq})\mathbf{e}_i, \tag{C12}$$

and summing over i, one obtains

$$\frac{\partial}{\partial t}\left(\sum_{i=0}^{8} f_i^{eq}\mathbf{e}_i\right) + \nabla\cdot\sum_{i=0}^{8} f_i^{eq}(\mathbf{e}_i\otimes\mathbf{e}_i) - \left(\sum_{i=0}^{8} F_i\mathbf{e}_i\right) = -\frac{1}{\varpi_f}\sum_{i=0}^{8}\mathbf{e}_i f_i^{(1)} + O(\varepsilon). \tag{C13}$$

Recalling [(C3), (C4), (C5), and (C7)], Eq. (C13) is obtained as

$$\frac{\partial}{\partial t}\left(\sum_{i=0}^{8} f_i^{eq}\mathbf{e}_i\right) + \nabla\cdot\sum_{i=0}^{8} f_i^{eq}(\mathbf{e}_i\otimes\mathbf{e}_i) - \left(\sum_{i=0}^{8} F_i\mathbf{e}_i\right) = -\frac{1}{\varpi}\sum_{i=0}^{8}\mathbf{e}_i f_i^{(1)} + O(\varepsilon). \tag{C14}$$

So, Eq. (C14) can be written as follows:

$$\rho\left[\frac{\partial\mathbf{u}}{\partial t} + (\mathbf{u}\cdot\nabla)\frac{\mathbf{u}}{\epsilon}\right] + \nabla(\epsilon p) - \frac{1}{\epsilon^{(n-1)}}\nabla.\boldsymbol{\tau} - \mathbf{F} = \mathbf{0} + O(\varepsilon), \tag{C15}$$

which demonstrates the generalized unsteady porous media for REV scale approach.

APPENDIX D: INTERNAL ENERGY DISTRIBUTION FUNCTION

The equation of the energy distribution function is as

$$\frac{\partial g_i}{\partial t} + \mathbf{e_i}\cdot\nabla_{\mathbf{x}} g_i - G_i = \frac{-1}{\varpi_g}\left(g_i - g_i^{eq}\right). \tag{D1}$$

The following conditions should be held to have the cited relation for the energy equilibrium distribution function $g_i^{eq}(\mathbf{x}, t)$

$$\sum_{i=0}^{8} g_i^{eq} = (\rho c_p)_m T, \tag{D2}$$

$$\sum_{i=0}^{8} g_i^{eq}\mathbf{e}_i = (\rho c_p)_f T\,\mathbf{u} + \mathbf{q} + \mathbf{q}' - \boldsymbol{\tau}\cdot\mathbf{u}, \tag{D3}$$

$$\sum_{i=0}^{8} G_i = \left[\frac{\mu}{K}\mathbf{u} + \frac{\rho E}{\sqrt{K}}\mathbf{u}|\mathbf{u}|\right]\cdot\mathbf{u} + (\nabla\cdot\boldsymbol{\tau})\cdot\mathbf{u}. \tag{D4}$$

The Chapman–Enskog expansion gives

$$g_i = g_i^{eq} + \varepsilon g_i^{(1)} + \varepsilon^2 g_i^{(2)} + O(\varepsilon^3). \tag{D5}$$

By substituting the relation in (D5) into (D1), we have

$$\frac{\partial g_i^{eq}}{\partial t} + \nabla\cdot(g_i^{eq}\mathbf{e}_i) - G_i = -\frac{1}{\varpi_g} g_i^{(1)} + O(\varepsilon). \tag{D6}$$

Summing Eq. (D6) over i,

$$\frac{\partial}{\partial t}\left(\sum_{i=0}^{8} g_i^{eq}\right) + \nabla\cdot\left(\sum_{i=0}^{8} g_i^{eq}\mathbf{e}_i\right) - \left(\sum_{i=0}^{8} G_i\right) = -\frac{1}{\varpi_g}\sum_{i=0}^{8} g_i^{(1)} + O(\varepsilon). \tag{D7}$$

Using Eqs. (D2)–(D4), the above equation becomes

$$\frac{\partial}{\partial t}\left((\rho c_p)_m T\right) + \nabla\cdot\left((\rho c_p)_f T\mathbf{u} - \boldsymbol{\tau}\cdot\mathbf{u} + \mathbf{q} + \mathbf{q}'\right) - \left((\nabla\cdot\boldsymbol{\tau})\cdot\mathbf{u} - \left[\frac{\mu}{K}\mathbf{u} - \frac{\rho E}{\sqrt{K}}\mathbf{u}|\mathbf{u}|\right]\cdot\mathbf{u}\right) = 0 + O(\varepsilon). \tag{D8}$$

Equation (D8) can be written as

$$(\rho c_p)_m\frac{\partial T}{\partial t} + (\rho c_p)_f\mathbf{u}\cdot\nabla T + \nabla\cdot q + \nabla\cdot q' - \nabla\cdot(\boldsymbol{\tau}\cdot\mathbf{u}) + (\nabla\cdot\boldsymbol{\tau})\cdot\mathbf{u} - \left[\frac{\mu}{K}\mathbf{u} - \frac{\rho E}{\sqrt{K}}\mathbf{u}|\mathbf{u}|\right]\cdot\mathbf{u} = 0 + O(\varepsilon), \tag{D9}$$

where

$$\nabla\cdot(\boldsymbol{\tau}\cdot\mathbf{u}) - (\nabla\cdot\boldsymbol{\tau})\cdot\mathbf{u} = \frac{1}{2}\boldsymbol{\tau} : \mathbf{A_1}. \tag{D10}$$

So, we can have the following relationship.

$$-\nabla\cdot(\boldsymbol{\tau}\cdot\mathbf{u}) + (\nabla\cdot\boldsymbol{\tau})\cdot\mathbf{u} - \left[\frac{\mu}{K}\mathbf{u} - \frac{\rho E}{\sqrt{K}}\mathbf{u}|\mathbf{u}|\right]\cdot\mathbf{u} = -\frac{1}{2}\boldsymbol{\tau} : \mathbf{A_1} - \left[\frac{\mu}{K}\mathbf{u} - \frac{\rho E}{\sqrt{K}}\mathbf{u}|\mathbf{u}|\right]\cdot\mathbf{u} = -\Phi \tag{D11}$$

with considering $q = -k_e\frac{\partial T}{\partial \mathbf{x}}$ and $q' = -\frac{\rho D k_T}{c_s}\frac{\partial C}{\partial \mathbf{x}}$, and dividing by $(\rho c_p)_f$, Eq. (D9) becomes

$$\frac{(\rho c_p)_m}{(\rho c_p)_f}\frac{\partial T}{\partial t} + \mathbf{u}\cdot\nabla T - \nabla\cdot(\alpha_e\nabla T) - \nabla\cdot(D_{TC}\nabla C) - \Phi = 0 + O(\varepsilon). \tag{D12}$$

Equation (D12) satisfies Eq. (A7).

APPENDIX E: CONCENTRATION DISTRIBUTION FUNCTION

The equation of the concentration distribution function is as follows:

$$\frac{\partial h_i}{\partial t} + \mathbf{e_i}\cdot\nabla_{\mathbf{x}} h_i = \frac{-1}{\varpi_h}\left(h_i - h_i^{eq}\right). \tag{E1}$$

The following relations must hold:

$$\sum_{i=0}^{8} h_i^{eq} = \epsilon C, \tag{E2}$$

$$\sum_{i=0}^{8} h_i^{eq}\mathbf{e}_i = \mathbf{J} + \mathbf{J}'. \tag{E3}$$

The Chapman–Enskog expansion gives

$$h_i = h_i^{eq} + \varepsilon h_i^{(1)} + \varepsilon^2 h_i^{(2)} + O(\varepsilon^3). \tag{E4}$$

Substituting the expression for h_i in (E4) into Eq. (E1), and summing over i

$$\frac{\partial}{\partial t}\left(\sum_{i=0}^{8} h_i^{eq}\right) + \nabla \cdot \left(\sum_{i=0}^{8} h_i^{eq}\mathbf{e}_i\right) = -\frac{1}{\varpi_h}\sum_{i=0}^{8} h_i^{(1)} + O(\varepsilon) \cdot \quad \text{(E5)}$$

Using Eqs. (E2)–(E4), the above equation becomes

$$\frac{\partial}{\partial t}\epsilon C + \nabla \cdot (\mathbf{J} + \mathbf{J}') = 0 + O(\varepsilon), \quad \text{(E6)}$$

we have $\mathbf{J} = \mathbf{u}\,C - D_e \nabla C$ and $\mathbf{J}' = -D_{CT}\nabla T$, so Eq. (E6) can be written as

$$\frac{\partial}{\partial t}\epsilon C + \nabla \cdot (\mathbf{u}\,C) - \nabla \cdot (D_e \nabla C) - \nabla \cdot (D_{CT}\nabla T) = 0 + O(\varepsilon), \quad \text{(E7)}$$

where $\nabla \cdot (\mathbf{u}\,C) = \mathbf{u}\,\nabla C + C(\nabla \cdot \mathbf{u})$ Since the fluid flow is incompressible, the term of $\nabla \cdot \mathbf{u}$ is equal to zero. So, it concludes that $\nabla \cdot (\mathbf{u}\,C) \equiv \mathbf{u}\,\nabla C$. With this information, Eq. (E7) is presented as

$$\epsilon\frac{\partial C}{\partial t} + \mathbf{u} \cdot \nabla C - D_e \nabla^2 C - D_{CT}\nabla^2 T = 0 + O(\varepsilon), \quad \text{(E8)}$$

which demonstrates Eq. (A8).

DATA AVAILABILITY

The data that support the findings of this study are available from the corresponding author upon reasonable request.

REFERENCES

[1]K. Vafai, *Handbook of Porous Media* (Marcel Dekker, New York, 2005).
[2]D. B. Ingham and I. Pop, *Transport Phenomena in Porous Media* (Elsevier, Amsterdam, 1998).
[3]D. A. Nield and A. Bejan, *Convection in Porous Media*, 3th ed. (Springer, 2006).
[4]Y. Mahmoudi, K. Hooman, and K. Vafai, *Convection Heat Transfer in Porous Media* (CRC Press, 2019).
[5]P. Forchheimer, "Wasserbewegung durch Boden," Forsch. Ver. D. Ing. **45**, 1782–1788 (1901).
[6]S. Whitaker, "The Forchheimer equation: A theoretical development," Transp. Porous Media **25**, 27–61 (1996).
[7]H. C. Brinkman, "A calculation of the viscous force extended by a flowing fluid on a dense swarm of particles," J. Appl. Sci. Res. **Al**, 27–34 (1947).
[8]J. A. Ochoa-Tapia and S. Whitaker, "Momentum transfer at the boundary between a porous medium and a homogeneous fluid—I. Theoretical development," Int. J. Heat Mass Transfer **38**, 2647–2655 (1995).
[9]T. S. Lundgren, "Slow flow through stationary random beds and suspensions of spheres," J. Fluid Mech. **51**, 273–299 (1972).
[10]J. Rubinstein, "Effective equations for flow in random porous media with a large number of scales," J. Fluid Mech. **170**, 379–383 (1986).
[11]L. Durlofsky and J. F. Brady, "Analysis of the Brinkman equation as a model for flow in porous media," Phys. Fluids **30**, 3329–3341 (1987).
[12]K. Vafai and C. L. Tien, "Boundary and inertia effects on flow and heat transfer in porous media," Int. J. Heat Mass Transfer **24**, 195–203 (1981).
[13]D. A. Nield, "The limitations of the Brinkman–Forchheimer equation in modeling flow in a saturated porous medium and at an interface," Int. J. Heat Fluid Flow **12**, 269–272 (1991).
[14]S. Whitaker, "The equations of motion in porous media," Chem. Eng. Sci. **21**, 291–300 (1966).
[15]S. Whitaker, "Diffusion and dispersion in porous media," AIChE J. **13**, 420–427 (1967).
[16]S. Whitaker, "Advances in the theory of fluid motion in porous media," Ind. Eng. Chem. **61**, 14–28 (1969).
[17]K. Vafai and S. J. Kim, "On the limitations of the Brinkman–Forchheimer-extended equation," Int. J. Heat Fluid Flow **16**, 11–15 (1995).
[18]K. Vafai, "Convection flow and heat transfer in variable-porosity media," J. Fluid Mech. **147**, 233–259 (1984).
[19]G. Lauriat and V. Prasad, "Natural convection in a vertical porous cavity: a numerical study for Brinkman-extended Darcy formulation, natural convection in porous media," J. Heat Transfer **56**, 13–23 (1986).
[20]C. T. Hsu and P. Cheng, "Thermal dispersion in a porous medium," Int. J. Heat Mass Transfer **33**, 1587–1597 (1990).
[21]P. Nithiarasu, K. N. Seetharamu, and T. Sundararajan, "Natural convection heat transfer in a fluid saturated variable porosity medium," Int. J. Heat Mass Transfer **40**, 3955–3967 (1997).
[22]P. Nithiarasu and K. Ravindran, "A new semi-implicit time stepping procedure for buoyancy driven flow in a fluid saturated porous medium," Comput. Methods Appl. Mech. Eng. **165**, 147–154 (1998).
[23]D. B. Ingham, I. Pop, and P. Cheng, "Combined free and forced convection in a porous medium between two vertical walls with viscous dissipation," Transp. Porous Media **5**, 381–398 (1990).
[24]D. A. Nield, "Resolution of a paradox involving viscous dissipation and nonlinear drag in porous medium," Transp. Porous Media **41**, 349–357 (2000).
[25]A. K. Al-Hadhrami, L. Elliott, and D. B. Ingham, "A new model for viscous dissipation across a range of permeability values," Transp. Porous Media **53**, 117–122 (2003).
[26]S. Chakraborty, "Dynamics of capillary flow of blood into a microfluidic channel," Lab Chip **5**, 421–430 (2005).
[27]C. Ancey, "Plasticity and geophysical flows: A review," J. Non-Newtonian Fluid Mech. **142**, 4–35 (2007).
[28]M. Iasiello, K. Vafai, A. Andreozzi, and N. Bianco, "Low-density lipoprotein transport through an arterial wall under hyperthermia and hypertension conditions—An analytical solution," J. Biomech. **49**, 193–204 (2016).
[29]K. Khanafer and K. Vafai, "The role of porous media in biomedical engineering as related to magnetic resonance imaging and drug delivery," Heat Mass Transfer **42**, 939–953 (2006).
[30]A. A. Osiptsov, "Fluid mechanics of hydraulic fracturing: A review," J. Pet. Sci. Eng. **156**, 513–535 (2017).
[31]R. Barati and J.-T. Liang, "A review of fracturing fluid systems used for hydraulic fracturing of oil and gas wells," J. Appl. Polym. Sci. **131**, 40735 (2014).
[32]T. Sochi, "Non-Newtonian flow in porous media," Polymer **51**, 5007–5023 (2010).
[33]R. B. Bird, W. E. Stewart, and, and E. N. Lightfoot, *Transport Phenomena* (Wiley, New York, 1960).
[34]R. H. Christopher and S. Middleman, "Power-law flow through a packed tube," Ind. Eng. Chem. Fundam. **4**, 422–426 (1965).
[35]J. G. Savins, "Non-Newtonian flow through porous media," Ind. Eng. Chem. **61**, 18–47 (1969).
[36]Z. Kemblowski and M. Michniewicz, "A new look at the laminar flow of power-law fluids through granular beds," Rheol. Acta **18**, 730–739 (1979).
[37]H. Pascal, "Non-steady flow of non-Newtonian fluids through a porous medium," Int. J. Eng. Sci. **21**, 199–210 (1983).
[38]R. V. Dharmadhikari and D. D. Kale, "Flow of non-Newtonian fluids through porous media," Chem. Eng. Sci. **40**, 527–529 (1985).
[39]B. Amari, P. Vasseur, and E. Bilgen, "Natural convection of a non-Newtonian fluid in a horizontal porous layer," Heat Mass Transfer **29**, 185–193 (1994).
[40]D. Getachew, W. J. Minkowycz, and D. Poulikakos, "Natural convection in a porous cavity saturated with a non-Newtonian fluid," J. Thermophys. Heat Transfer **10**, 640–651 (1996).
[41]J. R. A. Pearson and P. M. J. Tardy, "Models for flow of non-Newtonian and complex fluids through porous media," J. Non-Newtonian Fluid Mech. **102**, 447–473 (2002).
[42]J.-L. Auriault, P. Royer, and C. Geindreau, "Filtration law for power-law fluids in anisotropic porous media," Int. J. Eng. Sci. **40**, 1151–1163 (2002).
[43]S. Woudberg, J. P. D. Plessis, and G. J. F. Smit, "Non-Newtonian purely viscous flow through isotropic granular porous media," Chem. Eng. Sci. **61**, 4299–4308 (2006).
[44]A. Barletta and D. A. Nield, "Linear instability of the horizontal through flow in a plane porous layer saturated by a power-law fluid," Phys. Fluids **23**, 013102 (2011).
[45]L. Alves and A. Barletta, "Convective instability of the Darcy–Bénard problem with through flow in a porous layer saturated by a power-law fluid," Int. J. Heat Mass Transfer **62**, 495–506 (2013).

[46]S. Longo, V. D. Federico, L. Chiapponi, and R. Archetti, "Experimental verification of power-law non-Newtonian axisymmetric porous gravity currents," J. Fluid Mech. **731**, R2 (2013).
[47]A. Barletta and L. Storesletten, "Linear instability of the vertical through flow in a horizontal porous layer saturated by a power-law fluid," Int. J. Heat Mass Transfer **99**, 293–302 (2016).
[48]A. V. Shenoy, "Darcy–Forchheimer natural, forced and mixed convection heat transfer in non-Newtonian power-law fluid-saturated porous media," Transp. Porous Media **11**, 219–241 (1993).
[49]A. V. Shenoy, "Non-Newtonian fluid heat transfer in porous media," Adv. Heat Transfer **15**, 143–225 (1994).
[50]S. Chen and G. D. Doolen, "Lattice Boltzmann method for fluid flows," Annu. Rev. Fluid Mech. **30**, 329–364 (1998).
[51]S. Succi, *The Lattice Boltzmann Equation: For Fluid Dynamics and Beyond* (Oxford University Press, 2001).
[52]A. A. Mohamad, *Lattice Boltzmann Method: Fundamentals and Engineering Applications with Computer Codes* (Springer, 2011).
[53]Z. Chen, C. Shu, L. M. Yang, X. Zhao, and N. Y. Liu, "Immersed boundary-simplified thermal lattice Boltzmann method for incompressible thermal flows," Phys. Fluids **32**, 013605 (2020).
[54]O. Ilyin, "Gaussian lattice Boltzmann method and its applications to rarefied flows," Phys. Fluids **32**, 012007 (2020).
[55]Q. Li, Z. Lu, D. Zhou, X. Niu, T. Guo, and B. Du, "Unified simplified multiphase lattice Boltzmann method for ferrofluid flows and its application," Phys. Fluids **32**, 093302 (2020).
[56]Y. Zong, C. Zhang, H. Liang, L. Wang, and J. Xu, "Modeling surfactant-laden droplet dynamics by lattice Boltzmann method," Phys. Fluids **32**, 122105 (2020).
[57]G. Farag, S. Zhao, T. Coratger, P. Boivin, G. Chiavassa, and P. Sagaut, "A pressure-based regularized lattice-Boltzmann method for the simulation of compressible flows," Phys. Fluids **32**, 066106 (2020).
[58]L. Xu, X. Yu, and K. Regenauer-Lieb, "An immersed boundary-lattice Boltzmann method for gaseous slip flow," Phys. Fluids **32**, 012002 (2020).
[59]Z. Guo, B. Shi, and N. Wang, "Lattice BGK model for incompressible Navier–Stokes equation," J. Comput. Phys. **165**, 288–306 (2000).
[60]F. Verhaeghe, B. Blanpain, and P. Wollants, "Lattice Boltzmann method for double-diffusive natural convection," Phys. Rev. E **75**, 046705 (2007).
[61]X. Yu, Z. Guo, and B. Shi, "Numerical study of cross diffusion effects on double diffusive convection with lattice Boltzmann method," in International Conference on Computational Science —ICCS (2007), pp. 810–817.
[62]Z. Chai and T. S. Zhao, "Lattice Boltzmann model for the convection-diffusion equation," Phys. Rev. E **87**, 063309 (2013).
[63]A. A. Mohamad, R. Bennacer, and M. El-Ganaoui, "Double dispersion, natural convection in an open end cavity simulation via lattice Boltzmann method," Int. J. Therm. Sci. **49**, 1944–1953 (2010).
[64]Z. Guo and T. S. Zhao, "Lattice Boltzmann model for incompressible flows through porous media," Phys. Rev. E **66**, 036304 (2002).
[65]Z. Guo and T. S. Zhao, "Lattice Boltzmann model for incompressible flows through porous media," Numer. Heat Transfer B **47**, 157–177 (2005).
[66]Q. Liu, Y. He, Q. Li, and W. Tao, "A multiple-relaxation-time lattice Boltzmann model for convection heat transfer in porous media," Int. J. Heat Mass Transfer **73**, 761–775 (2014).
[67]L. Wanga, J. Mi, and Z. Guo, "A modified lattice Bhatnagar–Gross–Krook model for convection heat transfer in porous media," Int. J. Heat Mass Transfer **94**, 269–291 (2016).
[68]D. Gao, Z. Chen, and L. Chen, "A thermal lattice Boltzmann model for natural convection in porous media under local thermal non-equilibrium conditions," Int. J. Heat Mass Transfer **70**, 979–989 (2014).
[69]D. Gao, Z. Chen, L. Chen, and D. Zhang, "A modified lattice Boltzmann model for conjugate heat transfer in porous media," Int. J. Heat Mass Transfer **105**, 673–683 (2017).
[70]S. Chen, B. Yang, and C. Zheng, "Simulation of double diffusive convection in fluid-saturated porous media by lattice Boltzmann method," Int. J. Heat Mass Transfer **108**, 1501–1510 (2017).
[71]E. S. Boek, J. Chin, and P. V. Coveney, "Lattice Boltzmann simulation of the flow of non-Newtonian fluids in porous media," Int. J. Mod. Phys. B **17**, 99–102 (2003).
[72]S. Gabbanelli, G. Drazer, and J. Koplik, "Lattice Boltzmann method for non-Newtonian (power-law) fluids," Phys. Rev. E **72**, 046312 (2005).
[73]S. P. Sullivan, L. F. Gladden, and M. L. Johns, "Simulation of power-law fluid flow through porous media using lattice Boltzmann techniques," J. Non-Newtonian Fluid Mech. **133**, 91–98 (2006).
[74]J. Boyd, J. Buick, and S. Green, "A second-order accurate lattice Boltzmann non- Newtonian flow model," J. Phys. A: Math. Gen. **39**, 14241–14247 (2006).
[75]S. P. Sullivan, A. J. Sederman, M. L. Johns, and L. F. Gladden, "Verification of shearthinning LB simulations in complex geometries," J. Non-Newtonian Fluid Mech. **143**, 59–63 (2007).
[76]J. Psihogios, M. E. Kainourgiakis, A. G. Yiotis, A. Papaioannou, and A. K. Stubos, "A lattice Boltzmann study of non-Newtonian flow in digitally reconstructed porous domains," Trans. Porous Media **70**, 279–292 (2007).
[77]L. Velázquez-Ortega and S. Rodríguez-Romo, "Local effective permeability distributions for non-Newtonian fluids by the lattice Boltzmann equation," Chem. Eng. Sci. **64**, 2866–2880 (2009).
[78]X. He, S. Chen, and G. D. Doolen, "A novel thermal model for the lattice Boltzmann method in incompressible limit," J. Comput. Phys. **146**, 282–300 (1998).
[79]Y. Shi, T. S. Zhao, and Z. L. Guo, "Thermal lattice Bhatangar–Gross–Krook model for flows with viscous heat dissipation in the incompressible limit," Phys. Rev. E **70**, 066310 (2004).
[80]S. C. Fu, W. W. F. Leung, and R. M. C. So, "A lattice Boltzmann method based numerical scheme for microchannel Flows," J. Fluids Eng. **131**, 081401 (2009).
[81]S. C. Fu and R. M. C. So, "Modeled lattice Boltzmann equation and the constant-density assumption," AIAA J. **47**, 3038–3042 (2009).
[82]S. C. Fu, R. M. C. So, and R. M. C. Leung, "Linearized-Boltzmann-type-equation-based finite difference method for thermal incompressible flow," Comput. Fluids **69**, 67–80 (2012).
[83]R. R. Huilgol and G. H. R. Kefayati, "From mesoscopic models to continuum mechanics: Newtonian and non-newtonian fluids," J. Non Newtonian Fluid Mech. **233**, 146–154 (2016).
[84]R. R. Huilgol and G. H. R. Kefayati, "A particle distribution function approach to the equations of continuum mechanics in Cartesian, cylindrical and spherical coordinates: Newtonian and non-Newtonian fluids," J. Non-Newtonian Fluid Mech. **251**, 119–131 (2018).
[85]G. R. Kefayati, H. Tang, A. Chan, and X. Wang, "A Lattice Boltzmann model for thermal non-Newtonian fluid flows through porous media," Comput. Fluids **176**, 226–244 (2018).
[86]E. F. Toro, *Riemann Solvers and Numerical Methods for Fluid Dynamics: A Practical Introduction* (Springer, 1999), pp. 531–542.
[87]B. Goyeau, J.-P. Songbe, and D. Gobin, "Numerical study of double-diffusive natural convection in a porous cavity using the Darcy–Brinkman formulation," Int. J. Heat Mass Transfer **39**, 1363–1378 (1996).
[88]G. Lauriat and V. Prasad, "Non-Darcian effects on natural convection in a vertical porous enclosure, natural convection in porous media," Int. J. Heat Mass Transfer. **32**, 2135–2148 (1989).
[89]D. Das, P. Biswal, M. Roy, and T. Basak, "Role of the importance of Forchheimer term for visualization of natural convection in porous enclosures of various shapes," Int. J. Heat Mass Transfer **97**, 1044–1068 (2016).
[90]D. Das and T. Basak, "Role of discrete heating on the efficient thermal management within porous square and triangular enclosures via heatline approach," Int. J. Heat Mass Transfer **112**, 489–508 (2017).
[91]I. Sezai and A. A. Mohamad, "Three-dimensional double-diffusive convection in a porous cubic enclosure due to opposing gradients of temperature and concentration," J. Fluid Mech. **400**, 333–353 (1999).
[92]O. Kvernvold and P. Tyvand, "Thermal convection in anisotropic porous media," J. Fluid Mech. **90**, 609–624 (1979).
[93]L. Storesletten, "Natural convection in a horizontal porous layer with anisotropic thermal diffusivity," Transp. Porous Media **12**, 19–29 (1993).
[94]W. Bian, P. Vasseur, and E. Bilgen, "Boundary-layer analysis for natural convection in a vertical porous layer filled with a non-Newtonian fluid," Int. J. Heat Fluid Flow **15**, 384–391 (1994).

[95]A. Shenoy, *Heat Transfer to non-Newtonian Fluids: Fundamentals and Analytical Expressions* (John Wiley & Sons, 2018).
[96]P. V. Brandao, M. Celli, A. Barletta, and L. Storesletten, "Thermally unstable through flow of a power-law fluid in a vertical porous cylinder with arbitrary cross-section," Int. J. Therm. Sci. **159**, 106616 (2021).
[97]C. Chahtour, H. Ben Hamed, H. Beji, A. Guizani, and W. Alimi, "Convective hydromagnetic instabilities of a power-law liquid saturating a porous medium: Flux conditions," Phys. Fluids **30**, 013101 (2018).
[98]N. Khelifa, Z. Alloui, H. Beji, and P. Vasseur, "Natural convection in a vertical porous cavity filled with a non-Newtonian binary fluid," AIChE J. **58**, 1704–1716 (2012).
[99]N. Khelifa, Z. Alloui, H. Beji, and P. Vasseur, "Natural convection in a horizontal porous cavity filled with a non-Newtonian binary fluid of power-law type," J. Non-Newtonian Fluid Mech. **169–170**, 15–25 (2012).
[100]G. Kim, J. Hyun, and H. S. Kwak, "Transient buoyant convection of a power law Non-Newtonian fluid in an enclosure," Int. J. Heat Mass Transfer **46**, 3605–3617 (2003).
[101]O. Turan, A. Sachdeva, R. J. Poole, and N. Chakraborty, "Laminar natural convection of power-law fluids in a square enclosure with differentially heated sidewalls subjected to constant wall heat flux," J. Heat Transfer **134**, 122504 (2012).
[102]O. Turan, A. Sachdeva, N. Chakraborty, and R. J. Poole, "Laminar natural convection of power-law fluids in a square enclosure with differentially heated side walls subjected to constant Temperatures," J. Non-Newtonian Fluid Mech. **166**, 1049–1063 (2011).
[103]C. Sasmal, A. K. Gupta, and R. P. Chhabra, "Natural convection heat transfer in a power-law fluid from a heated rotating cylinder in a square duct," Int. J. Heat Mass Transfer **129**, 975–996 (2019).
[104]A. K. Tiwari and R. P. Chhabra, "Laminar natural convection in power-law liquids from a heated semi-circular cylinder with its flat side oriented downward," Int. J. Heat Mass Transfer **58**, 553–567 (2013).
[105]K. Khanafer, A. AlAmiri, and J. Bull, "Laminar natural convection heat transfer in a differentially heated cavity with a thin porous fin attached to the hot wall," Int. J. Heat Mass Transfer **87**, 59–70 (2015).